BIOCHEMISTRY

 Volume 45, Number 2 January 17, 2006

Current Topics

Light Harvesting in Photosystem I Supercomplexes[†,‡]

Alexander N. Melkozernov,[*,§] James Barber,[||] and Robert E. Blankenship[§]

Department of Chemistry and Biochemistry and Center for the Study of Early Events in Photosynthesis, Arizona State University, Tempe, Arizona 85287-1604, and Wolfson Laboratories, Division of Molecular Biosciences, Imperial College, London SW7 2AY, U.K.

Received September 23, 2005; Revised Manuscript Received December 5, 2005

ABSTRACT: In photosynthetic membranes of cyanobacteria, algae, and higher plants, photosystem I (PSI) mediates light-driven transmembrane electron transfer from plastocyanin or cytochrome c_6 to the ferredoxin−NADP complex. The oxidoreductase function of PSI is sensitized by a reversible photooxidation of primary electron donor P700, which launches a multistep electron transfer via a series of redox cofactors of the reaction center (RC). The excitation energy for the functioning of the primary electron donor in the RC is delivered via the chlorophyll core antenna in the complex with peripheral light-harvesting antennas. Supermolecular complexes of the PSI acquire remarkably different structural forms of the peripheral light-harvesting antenna complexes, including distinct pigment types and organizational principles. The PSI core antenna, being the main functional unit of the supercomplexes, provides an increased functional connectivity in the chlorophyll antenna network due to dense pigment packing resulting in a fast spread of the excitation among the neighbors. Functional connectivity within the network as well as the spectral overlap of antenna pigments allows equilibration of the excitation energy in the depth of the whole membrane within picoseconds and loss-free delivery of the excitation to primary donor P700 within 20−40 ps. Low-light-adapted cyanobacteria under iron-deficiency conditions extend this capacity via assembly of efficiently energy coupled rings of CP43-like complexes around the PSI trimers. In green algae and higher plants, less efficient energy coupling in the eukaryotic PSI−LHCI supercomplexes is probably a result of the structural adaptation of the Chl *a*/*b* binding LHCI peripheral antenna that not only extends the absorption cross section of the PSI core but participates in regulation of excitation flows between the two photosystems as well as in photoprotection.

Photosynthesis is a fundamental biological process supplying Earth's biosphere with oxygen and energy for living organisms (*1*). Photosystems I and II (PSI[1] and PSII, respectively) are major parts of the molecular photosynthetic machinery in oxygenic cyanobacteria, algae, and higher plants. The two photosystems operate in a concerted way in

[†] This work was supported by NRI/CSREES/USDA Grant 2003-35318-13665 to A.N.M., NSF Grant MCB-9727607 to R.E.B., and a BBSRC grant to J.B.

[‡] This is publication 647 of the Center for the Study of Early Events in Photosynthesis at Arizona State University.

* To whom correspondence should be addressed: Department of Chemistry and Biochemistry, Arizona State University, Tempe, AZ 85287-1604. Phone: (480) 965-1437. Fax: (480) 965-2747. E-mail: Alexander.Melkozernov@asu.edu.

[§] Arizona State University.

[||] Imperial College.

[1] Abbreviations: Chl *a*, chlorophyll *a*; CP43, PsbC subunit of photosystem II; CP43′, iron-stressed induced protein encoded by the *isi*A gene; cryo-EM, electron cryomicroscopy; LHCI, peripheral light-harvesting complex of photosystem I; LHCII, peripheral light-harvesting complex of photosystem II; Pcb, light-harvesting proteins from oxyphotobacteria related to iron-stressed induced proteins; PSI, photosystem I; PSII, photosystem II; P700, primary electron donor in photosystem I; RC, reaction center.

10.1021/bi051932o CCC: $33.50
Published on Web 12/20/2005

thylakoid membranes. The major functions of PSII are photooxidation of water to oxygen and providing electrons and protons for the cytochrome b_6f (cyt b_6f) complex (*2*). The PSI complex accepts electrons from the cyt b_6f complex via plastocyanin or cytochrome c_6 and further catalyzes a light-driven transmembrane electron transfer to the ferredoxin−NADP complex, producing intracellular energy for carbon dioxide assimilation (*3*).

The oxidoreductase function of PSI is sensitized by a reversible photooxidation of primary electron donor P700, which launches a multistep electron transfer via a series of redox cofactors of the PSI reaction center (RC) (*3*, *4*). The excitation energy for the functioning of the primary electron donor in the PSI RC is delivered via a core antenna made up of chlorophyll (Chl) molecules bound to the protein. In contrast to most other photosynthetic systems, where the antennas and reaction centers are located on distinct complexes, PSI has a combined system in which the light-harvesting Chls are associated with the same protein that binds the redox cofactors of the electron transfer in the RC (*5*, *6*).

During the course of evolution, both PSI and PSII have acquired extrinsic or intrinsic peripheral light-harvesting antennas (LHC). The extension of light-harvesting capacity is identified by the fact that sunlight is a relatively dilute energy source. Even during a cloudless day the radiation flux of solar energy would result in absorption by each Chl molecule of only approximately 10 photons per second (*1*). Having the light-harvesting antennas allows photosynthetic organisms to avoid the reaction center idling while waiting for another photon. On the other hand, selective pressure during the evolution of the antenna complexes under changing environmental conditions was directed toward efficient delivery of the excitation energy to the RC before its dissipation (*7*). Undelivered or excess energy is harmful for photosystems since it is converted into the long-lived Chl triplet states capable of generating reactive singlet oxygen (*8*).

For PSI, Nature solved this dilemma by acquiring antennas with significant structural diversity ranging from externally coupled phycobilisomes (*9*, *10*) or integral membrane iron stress-induced Chl *a* binding proteins in cyanobacteria (*11*, *12*) to integral Chl *a*/*b* binding LHCI in green algae and higher plants (*13*−*17*). The remarkably different structural forms of the various antenna complexes of PSI, including distinct pigment types and organizational principles, strongly suggest that they have evolved independently in response to both the general need to increase the absorption cross section and the specific environmental conditions such as light quality, its intensity, nutrient availability, etc.

This review discusses the structure−function organization of light harvesting in PSI supercomplexes on the basis of recent structural and time-resolved spectroscopy studies of prokaryotic and eukaryotic systems.

I. PSI Core Antenna: A 100% Excitation Delivery to the Reaction Center through an Optimized Chlorophyll Antenna Network

Structural Organization of the PSI Core Light-Harvesting Antenna. The PSI core antenna is the central structural block of PSI supercomplexes. The detailed structure of the PSI core from the cyanobacterium *Thermosynechococcus elongatus* (former name *Synechococcus elongatus*) has been obtained by X-ray crystallography at 2.5 Å resolution (*6*; Protein Data Bank entry 1JB0). The monomeric PSI core complex consists of 12 protein subunits binding a significant amount of cofactors, including 96 chlorophyll *a* molecules, 22 β-carotenes, four lipids, three iron−sulfur clusters, and two phylloquinones (*6*) (Figure 1A). The largest transmembrane protein subunits, PsaA and PsaB, have a 43% amino-acid sequence identity and form a heterodimer. The heterodimer has two distinct structural domains related to the C- and N-termini of each protein. A palisade of five transmembrane helices in the C-terminal domain of PsaA and PsaB form a shell enclosing the electron transfer cofactors of the RC, six Chls, two phylloquinones, and three iron−sulfur centers (Figure 1B). Antenna pigments that transfer excitation energy to the C-terminal domains, including 85 of 96 antenna Chls of the PSI core (Figure 1C), are bound to the N-terminal domain presented by a bundle of six transmembrane helices. Peripheral PSI core subunits, PsaL, PsaK, PsaJ, PsaM, and PsaX, bind the remaining 11 Chls of the antenna.

The PsaA and PsaB subunits are related to each other by a 2-fold pseudosymmetry axis running in a transmembrane direction through the molecule of the primary donor in the RC in the lumenal part of the membrane and iron−sulfur cluster F_x on the stromal side. More than 80% of the Chls bound to the PSI core are related by this 2-fold pseudosymmetry with ∼60% conservation of the Chl-binding sites. Most of the Chls form two distinct layers at the stromal and lumenal sides of the thylakoid membrane (Figure 1D). Within each of the layers, Chls are arranged as distorted ellipses flanked at the distal ends by peripheral core antenna Chls (Figure 1C). The Chls in the antenna form a network since the average interpigment distance is comparable with the diameter of the Chl molecule (∼9 Å). The lumenal and stromal Chl ellipses are connected to each other via several Chls located in the middle of the membrane. Two of these Chls, a pair of symmetrical linkers, provide a structural connection of the stromal layer with the Chls in the RC (Figure 1C). A special structural feature of the PSI core is clustering of the pigments in the stromal and lumenal layers with a majority of the Chl clusters located within the pigment ellipses (*18*, *19*).

Prokaryotic and eukaryotic PSI core antennas seem to share the same location and orientation for the majority of Chls (*6*, *15*), which is governed by conservation of pigment-binding sites and protein folds.

Structural Features of PSI Trimers. In thylakoid membranes of cyanobacteria, PSI assembles as a trimer of identical core complexes (homotrimer) (Figure 2). The PsaL subunit of PSI is located in the trimer-forming domain, and its deletion prevents trimer formation (*20*, *21*). Each PsaL subunit is characterized by a specific structural rigidity (*22*), and the whole trimerization domain is reinforced by electrostatic and hydrophobic interactions among the transmembrane helices of neighboring PsaL subunits (*6*, *23*, *24*). Further stabilization of the trimer is maintained by interaction of PsaL with the peripheral PSI core subunits, PsaM and PsaI, as well as with the extrinsically docked PsaD subunit at the stromal side of the complex (*21*, *25*, *26*).

Because of the rigid structure of the PsaL trimerization domain, the number of pigment contacts between the monomers in the trimer is limited (*27*). Nevertheless, these

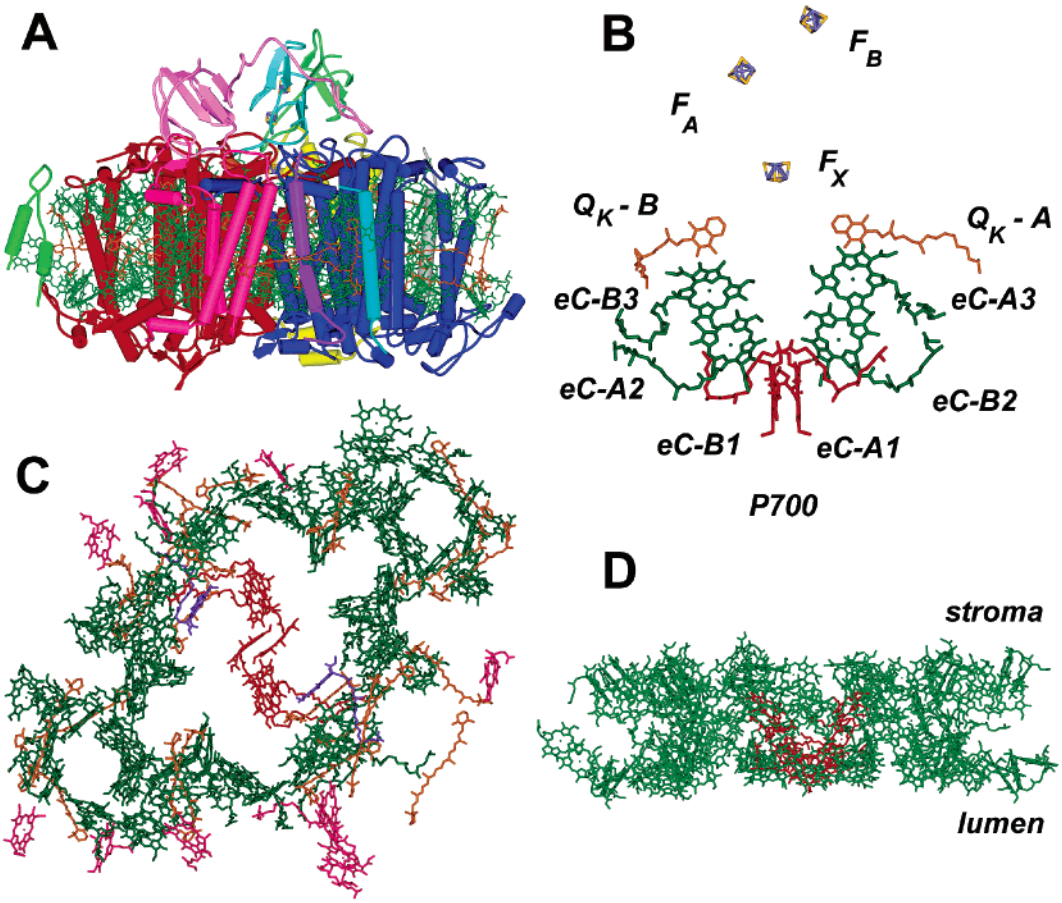

FIGURE 1: Structure of the photosystem I core from cyanobacteria. (A) Side view of the PSI core monomer consisting of nine intrinsic transmembrane and three extrinsic PSI subunits. (B) Side view of redox cofactors of electron transfer in the PSI RC, including two branches of electron carriers: eC-A1-eC-B1, excitation trap and primary donor P700; eC-A2 (eC-B2), accessory Chls; eC-A3 (eC-B3), primary acceptor A_0 and its symmetric counterpart; Q_K-A (Q_K-B), phylloquinones (secondary acceptors); F_X, F_A, and F_B, iron−sulfur clusters. (C) Top view of the PSI core pigment system: red for Chls in the RC, green for Chls bound to PsaA and PsaB subunits, magenta for Chls bound to peripheral PSI core subunits, and orange for β-carotene molecules. (D) Side view of the layer arrangement of the PSI core Chl antenna. Atomic coordinates of PSI from the cyanobacterium *S. elongatus* obtained from the Protein Data Bank [entry 1JB0 (*6*)]. Molecular graphics were rendered using Web Lab Viewer from Accelrys, Inc.

pigments seem to provide additional functional connections of three antenna networks in the PSI trimer (see below).

Principles of PSI Core Antenna Functioning. The PSI core monomer is the main functional unit of the cyanobacterial PSI trimer. It is also the best studied due to extensive time-resolved spectroscopy studies (reviewed in refs *28*−*31*) and the availability of a high-resolution crystal structure (*6*).

A dense packing of the pigments in the PSI core enhances the functional connectivity of the antenna via random sub-picosecond hopping of the excitations in the network (Figure 3). Time-resolved spectroscopy studies of the cyanobacterial PSI core reveals that the excitation energy transfer between the neighbors in the chlorophyll network occurs within 200−600 fs (*18*, *31*−35) (see Figure 3). Twenty-two β-carotene (Car) molecules embedded into the antenna network act as excitonic wires connecting carotenoids with Chls via ultrafast energy transfer, which predominantly occurs via the Car-S_2−Chl Q_y pathway (*36*−*38*) (see Figure 1C). Energy equilibration among the Chls occurs on the picosecond time scale (2−5 ps) and involves pools of the longest-wavelength absorbing (red) pigments (*18*, *33*, *39*−*43*). Similar conclusions have been made for the eukaryotic PSI core (*41*, *42*, *44*−*47*). The red spectral shift that is different in magnitude contributing to the spectral heterogeneity in the 670−710 nm region in PSI RCs from all organisms is a functional manifestation of the excitonic interactions in the pigment clusters (*32*, *33*). These interactions favor further spectral broadening and better overlap of the fluorescence with the absorption spectrum of primary donor P700 in the reaction center, which leads to efficient energy trapping within 20−40 ps. Three experimental time scales, i.e., sub-picosecond and picosecond energy equilibrations and photochemical trapping, unambiguously observed by time-resolved spectroscopy were successfully reproduced in recent modeling of the PSI excitation dynamics (*48*−*50*) based on the 2.5 Å resolution crystal structure (*6*).

Despite different modeling strategies (*19*, *27*, *48*−*51*), structure-based calculations generally agree about the clusters of the pigments with extreme red shifts. These pigments include symmetry-related dimers in the stromal layer of the PSI core located in the vicinity of connecting Chls, the PsaL adjacent cluster of Chls, and a trimer on the periphery of PsaB. The relative amount of red pigments is species-dependent (*31*, *35*, *41*, *43*) and is related to the presence of the Chl clusters on the periphery of the PSI core as well as those induced by trimerization (see below).

Major pools of red pigments in cyanobacterial and eukaryotic PSI seem to play similar roles due to similar orientations of a majority of core antenna Chls in both complexes (*6*, *15*). These pigments are structurally well

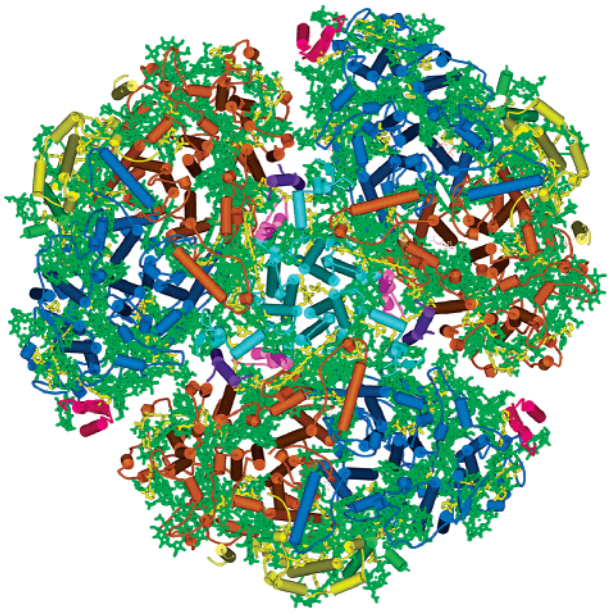

FIGURE 2: PSI trimer of identical core complexes (homotrimer) from cyanobacteria. The trimer is stabilized by the interaction of PsaL (colored light blue) with two transmembrane subunits, PsaM (purple) and PsaI (magenta), and an extrinsic subunit, PsaD (not shown). This figure was rendered using atomic coordinates of PSI from the cyanobacterium *S. elongatus* obtained at 2.5 Å resolution [PDB entry 1JB0 (*6*)].

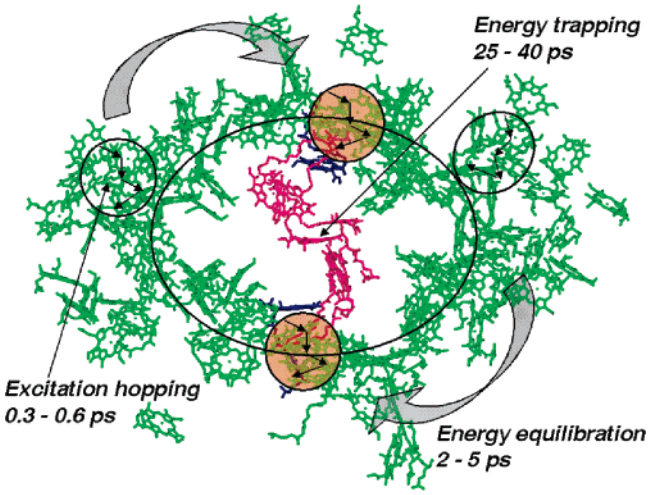

FIGURE 3: Functional organization of the PSI core antenna. Three experimental time scales in the excitation dynamics include random sub-picosecond hopping of the excitations in the antenna network, picosecond energy equilibration among Chls with different site energies, and overall decay of the excitation via energy trapping. Shaded circles indicate locations of the Chl clusters, most probable candidates for the red pigments. Chls in the RC and connecting Chls are colored red and purple, respectively. See the text for details.

integrated into the Chl core network (Figure 3); therefore, they not only enhance the absorption cross section of PSI but also function as transient traps gathering the excitation around the reaction center on the picosecond time scale (*18*, *32*, *48*, *52*, *53*). Excitation of the red pigments in the PSI core from *Synechocystis* sp. PCC6803 at 710 nm was shown to induce an ultrafast (0.4−0.7 ps) uphill energy transfer, suggesting the functional connectivity of the red pigments (presumably A38−A37 or B37−B38 dimers) via linkers to the Chls of the RC (*18*, *43*).

The photochemical trapping in the PSI core (20−40 ps) is independent of the excitation wavelength (*18*, *40*, *41*, *43*), but there is no overall agreement about how to interpret this experimental fact. In a trap-limited interpretation, kinetic processes in the RC would limit the overall decay of the excitation in the PSI core antenna (*18*, *41*, *42*, *54*, *55*). Structural coupling of the Chl antenna network and the redox active Chls in the RC via connecting chlorophylls (linkers) allows excitations to make multiple visits to the trap before the photochemical quenching due to the primary charge separation in the RC. In a transfer-to-trap limited interpretation, the overall distance between the PSI core antenna network and the exciton trap, P700, as well as the number of red pigments in the antenna determines the observed photochemical trapping (*30*). Recent structure-based kinetic modeling studies appear to reconcile both approaches concluding that both transfer-to-trap and trap-limited excitation dynamics are equally responsible for the observed trapping time (*19*, *48*, *49*).

The PSI core antenna network has an optimal design in terms of site energies and orientations of Chls (*19*, *48*, *49*). Linking Chls and red pigments seems to add to the optimal design of the network, slightly enhancing energy transfer from the core antenna to P700. A functionally connected Chl network results in a robustness of the excitation dynamics in the PSI core, and many routes of the excitation to P700 are possible. Organization of the antenna Chls in the PSI core is on the whole conserved between cyanobacteria and higher plants, suggesting that an optimization of the PSI light-harvesting system was attained more than 1 billion years ago (*56*).

Functions of the PSI Trimers. Spectroscopic differences between the PSI trimers and monomers are related to the presence of extremely low-energy red pigments induced by trimerization with a species-dependent magnitude of the effect. PSI trimers from *Synechocystis* sp. PCC6803 possess approximately five red Chls (*35*) with two spectral forms contributing to the red-most absorption band at 708 nm. The PSI core monomers demonstrate weak interactions in the trimer (*57*), which indicates that the red pigments are located within the pigment ellipse of the PSI core network (see Figure 3). As a result, no differences in the excitation dynamics are observed in the PSI trimers and monomers from this species (*18*, *35*, *39*, *40*, *43*, *58*, *59*). PSI trimers from *T. elongatus* bind approximately nine red Chls (*35*), absorbing at 708 and 719 nm and emitting at 730 nm at low temperatures. Monomerization of the trimer results in a significant decrease in absorption of the red-most spectral form, C-719, which supposedly originates from pigment−pigment interactions in clusters of pigments adjacent to PsaL (*35*, *60*). In a cyanobacterium *Arthrospira platensis* (former name *Spirulina platensis*), PSI is thought to form a very stable PSI trimer (*61*). In addition to the spectral form at 708 nm, which is contributed by absorption of approximately seven Chls of the PSI core monomer, there is in this organism an extremely red-shifted trimerization-induced spectral form at 740 nm giving rise to a 760 nm fluorescence at low temperatures (*24*, *35*, *62*).

Overall, on the basis of the results of time-resolved studies, the fast excitation dynamics of PSI trimers are dominated by the kinetic processes in individual PSI monomers. However, the photochemical trapping, which occurs in the fully equilibrated core antenna, slows with the increase of

the number of low-energy pigments. The lifetimes vary from 25 ps in PSI from *Synechocystis* irrespective of trimerization state (*18*, *35*, *40*, *59*) to 37 and 50 ps for the PSI monomers and PSI trimers, respectively, from *A. platensis* (*35*). An increase in the trapping time in the PSI trimers is likely to be associated with the presence in the trimer's excitation dynamics of additional excitation energy equilibration among the red pigments (*35*, *43*) or energy exchange among the pools of red pigments of neighboring monomers (*61*, *63*). Kinetic modeling based on the structure of PSI trimers (*27*) indicated the possibility of ultrafast energy transfer among the monomers within the trimer through several connecting pigments.

The possible functional significance of the PSI trimerization is puzzling since the P700:Chl ratio in monomers and trimers is the same and trapping capacities of P700 and $P700^+$ are similar (*39*, *64*). However, trimerization-induced red pigments extend the absorption cross section of the PSI complex further to the red spectral region (see above). PSI trimers are suggested to provide structural stabilization of the PSI peripheral subunits (*27*) or supercomplexes of the PSI with peripheral antenna, such as phycobilisomes (*23*, *27*) or iron stress-induced CP43′ antenna (*11*, *12*). Trimerization of PSI is also a feature of the cyanobacterial-related oxyphotobacteria such as *Prochlorococcus* and *Prochlorothrix*, which also have a CP43′-like antenna system composed of Chl *a*- and Chl *b*-binding Pcb proteins (*65*−*67*; see below).

In summary, functional connectivity in the PSI core antenna network due to dense pigment packing results in a fast spread of the excitation among the neighbors. Functional connectivity within the network as well as the spectral overlap of antenna pigments allows equilibration of the excitation energy in the depth of the whole membrane within picoseconds and loss-free delivery of the excitation to primary donor P700 within 20−50 ps.

II. PSI−CP43′ Supercomplex: Increase of Light-Harvesting Capacity under Low-Light and Iron-Deficiency Conditions

Structural Features of PSI−CP43′ Supercomplexes. Cyanobacteria are major producers of oxygen in the Earth's biosphere. During adaptive evolution, this group of photosynthetic microorganisms acquired different survival strategies, resulting in a dynamic rearrangement of the light-harvesting antennas coupled to PSII and PSI. One example of the regulation of light-harvesting capacity is the change in the extent and structure of phycobilisomes that allow cyanobacteria and red algae to respond to their environmental conditions (*68*, *69*). Such a response occurs when cyanobacteria are exposed to a limiting supply of iron, a common occurrence in their natural environment (*70*). Iron deficiency in cyanobacteria results in a significant decrease in phycobiliprotein content (*71*) and overall reduction of the PSI level relative to that of PSII (*72*). These changes seem, in part, to be compensated by the accumulation of the IsiA protein (CP43′) encoded by the "iron stress-induced" *isi*A genes (*73*−*75*). Accumulation of proteins that are homologous with IsiA proteins also occurs in the Chl *b*- and Chl *d*-containing oxyphotobacteria (*76*), suggesting that the observed phenomenon might be an example of a different survival strategy in adaptive evolution of the photosynthetic supercomplexes (*77*, *78*).

Recently, two laboratories have discovered that CP43′ and the PSI reaction center trimer from cyanobacteria form a supercomplex with a molecular mass of approximately 2 MDa (*11*, *12*, *79*). Electron microscopy studies confirmed that the accumulated protein assembles as a ring around the PSI trimer (Figure 4A). The available X-ray structures of the cyanobacterial PSI trimer (*6*) (Figure 2) and of CP43 from a PSII complex (*80*) have been satisfactorily modeled into a three-dimensional structure of the PSI−CP43′ supercomplex derived from electron cryomicroscopy (*81*). On the basis of this structure and earlier modeling (*11*, *79*), the CP43′ ring was shown to be composed of 18 copies of the protein. In oxyphotobacteria, CP43′-like Pcb proteins have been found to form similar ring structures around the PSI trimers (*65*, *67*, *83*). Moreover, in these oxyphotobacteria, the Pcb proteins, unlike CP43′, also form outer light-harvesting systems for PSII (*66*, *82*, *84*).

The CP43′ protein is a Chl *a*-binding protein having an amino acid sequence and spatial topology similar to those of CP43 from PSII (*11*, *85*) (Figure 4B,C). Available crystal structures of PSII (*80*, *86*, *87*) demonstrate that the protein part of the CP43 subunit (PsbC) of the PSII complex has a domain organization characterized by three distinct pairs of transmembrane helices (Figure 4C). This folding pattern is remarkably conserved among CP43, CP47 in PSII, and N-terminal antenna domains of PsaA and PsaB in PSI (*87*−*90*). Because of sequence similarities, the organization of Chls in CP43 is most likely to be shared with the Chls of CP43′ from cyanobacteria as well as with Chls of Pcb light-harvesting proteins from oxyphotobacteria (*76*). A 3.5 Å resolution model of CP43 (*87*) identified 14 Chl *a* molecules bound to the protein. Pigments are arranged in two layers with eight Chls in a lumenal layer, five Chls in a stromal layer, and one Chl located in the middle of the membrane, connecting the two layers. Eleven of 14 Chls have protein ligands conserved among both CP43 and CP43′, while three Chls seem to be stabilized by either pigment−pigment or indirect pigment−protein interactions. Sequence alignments of CP43 and the iron stress-induced proteins from different cyanobacteria indicate the presence of some conserved His residues among CP43′ that are not observed in CP43, suggesting that CP43′ binds an extra Chl *a* via the conserved histidine located in helix IIII. The three other additional histidines found in the loop regions of CP43′, and not in CP43, might also be chlorophyll binding sites.

In PSII, transmembrane helices V and VI of the CP43 protein are involved in interaction with the adjacent D1 subunit of the PSII reaction center (*87*). Similarly, it is likely that in the PSI−CP43′ supercomplex these helices in each CP43′ subunit are oriented toward the membrane-exposed surface of the PSI trimer (Figure 4C). The shape of the outer CP43′ ring in the PSI supercomplex is not exactly circular but rather distorted by interactions of the subunits with the PSI trimer. At the level of current resolution, it is difficult to predict the specificity of these interactions. Recently, it was shown that iron-depleted cells of *Synechocystis* sp. PCC6803 that lack the trimer-forming domain (PsaL) were able to maintain functional association of CP43′ and the PSI monomer (*91*). In this complex, six or seven subunits of CP43′ were associated along the edge of the PSI monomer. For each PSI monomer in the PSI−CP43′ supercomplex, there are three regions where the Chls in CP43′ are located

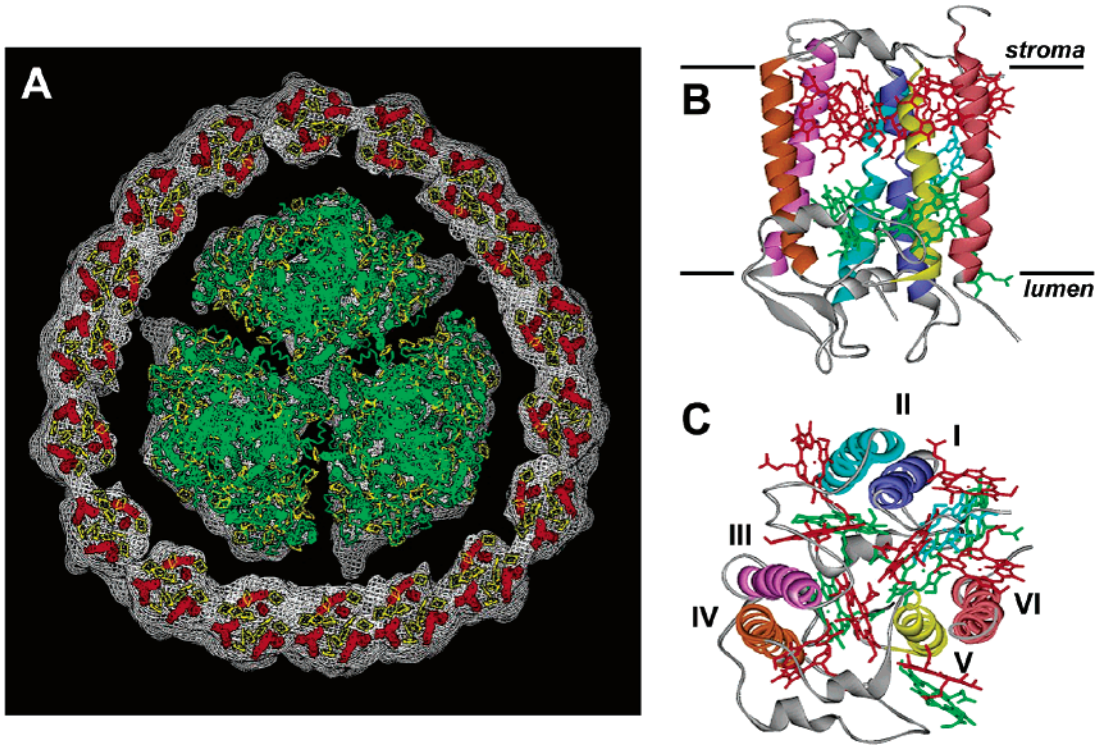

FIGURE 4: Structural model of the PSI supercomplex from iron-depleted cyanobacteria. (A) Low-resolution structural model of the PSI−CP43′ supercomplex based on electron cryomicroscopy (*81*). The photosystem I trimer is surrounded by 18 copies of the iron stress-induced CP43-like antenna pigment protein. (B) Side view of CP43 from photosystem II [PDB entry 1S5L (*87*)] showing six transmembrane helices binding 14 Chl *a* molecules arranged in lumenal (green) and stromal (red) layers. (C) Top view of CP43 with three pairs of transmembrane helices. Helices V and VI in CP43′ proteins are suggested to interact with the surface of the PSI core. See the text for details.

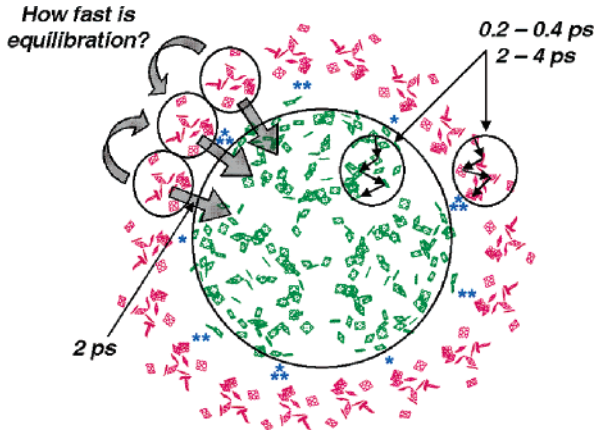

FIGURE 5: Functional organization of the PSI−CP43′ supercomplexes from cyanobacteria. Excitation dynamics of the PSI trimer (large circle) are dominated by the processes occurring in the PSI monomers (see Figure 3). Interactions of the CP43′ proteins in the ring with the PSI trimer (indicated by asterisks) as well as an energy gradient between Chls in CP43′ and the PSI core determine a fast energy transfer from peripheral antenna CP43′ and the PSI trimer.

closer to Chl *a* clusters in PsaA, PsaB, and PsaJ with interpigment distances of ~20−25 Å (*81*) (Figure 5). Interactions between the adjacent CP43′ subunits within the antenna ring seem to be tighter than those between the ring and the central PSI trimer (Figure 4A). An increased number of pigments in CP43′ could affect the interactions between CP43′ in the ring and between the ring and the PSI. Thus, the CP43′ organization in the antenna ring is stabilized primarily by interactions between adjacent CP43′ subunits, with a localized specific interaction with each PSI monomer.

Recently, Boekema and colleagues reported different structural states of aggregated CP43′ in *Synechocystis* cells with deleted PsaL or PsaF subunits in PSI (reviewed in ref *92*). Along with the assembly of the 18-mer CP43′ ring around the PSI trimer in wild-type cells, in the mutants CP43′ can form single or double rings around the monomeric PSI and can even exist as single or double rings without PSI. Formation of unusual ring structures is largely observed in the mutants after long iron starvation and might be related to a more complex physiological phenomenon such as a response to oxidative stress. These processes are far from being understood and are beyond the scope of this review (*78*, *92*).

Functioning of the PSI−CP43′ Supercomplexes in Cyanobacteria. In the cyanobacterial PSI−CP43′ supercomplexes, the major functions of the CP43′ ring are light harvesting and excitation energy transfer. In the supercomplex, ~290 Chl *a* molecules of the CP43′ ring contribute to the main absorption band at 673 nm while the pigments of the PSI reaction center including P700 absorb at 685−710 nm (*59*, *93*). Such a redistribution of the Chl *a* spectral forms amplified by an increase in light-harvesting capacity determines an efficient energy gradient from the peripheral antenna (CP43′) toward the PSI reaction center.

Recent time-resolved spectroscopy studies of the PSI−CP43′ supercomplexes from iron stress-induced cyanobacteria (*59*, *94*) concluded that the excitation energy transfer processes within the CP43′ ring and energy transfer from the CP43′ ring to the PSI core occur much faster than the photochemical trapping by the RC.

Despite the absence of reports on energy transfer studies of the isolated monomeric CP43′ protein, its structural similarity with CP43 would predict similar excitation energy transfer pathways (*95*). The structure of CP43 (Figure 4B,C) shows that interpigment distances between nearest neighbors in the stromal and lumenal layers of the protein favor sub-picosecond energy transfer (0.2−0.4 ps). Chls of the stromal layer appear to have stronger pigment−pigment interactions; therefore, they are likely to be involved in formation of the terminal emitter. Excitation equilibration among the Chls is in the direction toward the Chl(s) with the lowest energy (terminal emitter) and occurs on the picosecond time scale (2−4 ps).

In the CP43′ ring (Figures 4A and 5), these fast energy transfer processes would compete with the energy transfer among adjacent subunits and the energy transfer from CP43′ to the PSI core. The structural model predicts that the Chls in adjacent subunits can be as close as 10 Å from each other (*81*). Sub-picosecond connectivity within the Chl layers of CP43′ and tight interactions of adjacent CP43′ subunits could favor the ultrafast energy delocalization in the CP43′ ring. How many subunits are involved in this process would certainly depend on the energy transfer from the CP43′ ring to the PSI trimer, which occurs within ∼2 ps (*59*, *94*). The energy transfer pathways toward PSI run most possibly via closely located clusters of Chl *a* in CP43′ and suggested linker chlorophylls on the periphery of PsaA, PsaB, and PsaJ subunits in the PSI core (*79*, *81*) (Figure 5). On the basis of the Förster theory (*96*), the energy transfer time of ∼2 ps would correspond to an ∼20 Å separation between the excitation energy donor in CP43′ and the acceptor in PSI, in agreement with the distance estimated from the three-dimensional cryo-EM model of the PSI supercomplex (*81*).

The PSI−CP43′ supercomplex exhibits a longer photochemical trapping time (40 ps) compared to that in the PSI trimer (25 ps). This reflects the fact that the entire antenna in the PSI−CP43′ supercomplex is larger so that the fraction of time that the excitation is on the excitation trap (P700), and therefore available for trapping, is smaller.

Fast energy equilibration between CP43′ and the PSI trimer in cyanobacteria is an indication of efficient functional connectivity of the Chl network in the CP43′ ring to the antenna network of the PSI core resulting in a strong energy coupling of the supercomplex in agreement with the structural models. In such a network, there is no opportunity for energy dissipation as was shown to occur in uncoupled aggregates of CP43′ (*97*) since all excitation energy collected by the CP43′ rings around PSI in the iron-stressed low-light cells efficiently channels toward the RC.

A unilateral increase in light-harvesting capacity in PSI under low-light conditions due to assembly of rings of peripheral light-harvesting antennas consisting of either CP43′ or similar Pcb proteins would perturb the electron balance between the two photosystems in cyanobacteria. Recent discoveries of functional association of Pcb proteins with PSII (*66*, *82*, *84*) imply that the electron balance between PSI and PSII is maintained under low-light conditions by assembly of a CP43-like antenna in both PSI and PSII. The dynamic nature of this balance, however, might be associated with the presence of CP43-like proteins uncoupled from PSI in cyanobacterial thylakoids under iron starvation (*92*) as well as their mobility (*98*), suggesting that the complexes might participate in energy spillover between PSI and PSII under low-light conditions in cyanobacteria.

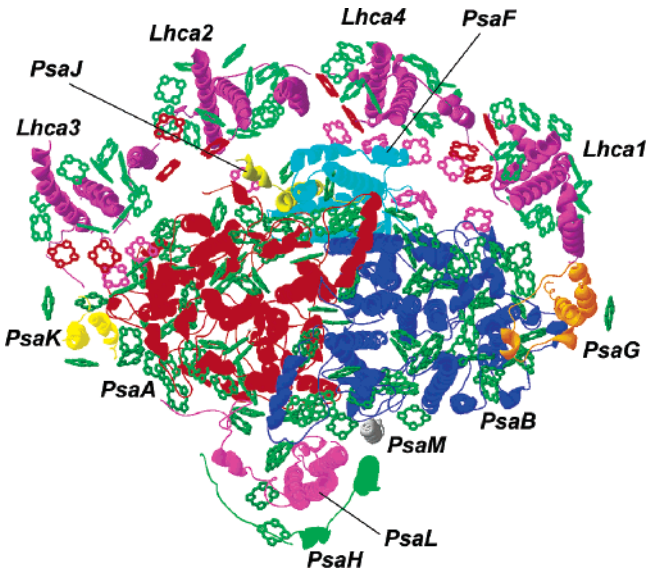

FIGURE 6: Structural model of the PSI−LHCI supercomplex from higher plants based on a 4.4 Å resolution crystal structure [PDB entry 1QZV (*15*)]. Top view perpendicular to the plane of the thylakoid membrane. The color code for the subunits follows: red for PsaA, blue for PsaB, light blue for PsaF, yellow-green for PsaJ, orange for PsaG, yellow for PsaK, magenta for PsaL, green for PsaH, and violet for LHCI subunits (Lhca1−Lhca4). The color code for chlorophylls follows: dark green for the PSI core antenna, light green for the peripheral antenna, red for Chl linkers in LHCI, and pink for gap pigments. For visualization of the subunits, the protein backbone was generated from the α-carbon atoms of the protein using the MaxSprout algorithm (*150*).

III. Eukaryotic PSI−LHCI Supercomplex: Striking a Balance between Efficient Energy Transfer and Regulation

The PSI complex in green algae and higher plants assembles as a monomer of the PSI core associated with the light-harvesting peripheral antenna, LHCI (*13*, *99*−*101*). The subunit complement of the eukaryotic PSI core complex is similar to that in cyanobacteria except for the presence of additional eukaryotic-specific protein subunits, PsaG, PsaN, PsaH, PsaO, and PsaP (*99*, *100*, *102*). LHCI from green algae and higher plants belongs to a related group of integral chlorophyll and carotenoid binding proteins with conserved pigment-binding sites and three distinct regions of transmembrane helices with largely similar protein folds (*10*, *53*, *103*−*107*). Biochemical, proteomics, and genomics studies of eukaryotic PSI indicate the presence of five to six distinct Lhca proteins in the LHCI from higher plants (*108*−*110*) and approximately seven to nine different Lhca proteins in the PSI peripheral antenna from the green alga *Chlamydomonas reinhardtii* (*111*−*115*).

Structure of the PSI−LHCI Complex from Higher Plants. The molecular structure of the PSI−LHCI complex from pea (*Pisum sativum*) has been obtained at 4.4 Å resolution using X-ray crystallography (*15*) (Figure 6). The structural model identifies four evenly spaced LHCI proteins, Lhca1, Lhca4, Lhca2, and Lhca3, attached to the PSI core complex on the side formed by the outer surface of the PsaG, PsaB, PsaF, PsaJ, PsaA, and PsaK subunits. Relatively weak protein−protein interactions between LHCI and the PSI core as well

Table 1: Summary of Chl Binding in the Cyanobacterial PSI Core (PDB entry 1JB0) and the PSI−LHCI Supercomplex from Pea (PDB entry 1QZV)

PSI subunit	no. of Chls in 1JB0	no. of Chls in 1QZV
	PsaA/PsaB	
RC	6	6
PsaA N-domain	40	40
PsaB N-domain	39	42
total	85	88
	Peripheral PSI Core Subunits	
PsaJ	3	2
PsaK	2	4
PsaL	3	4
PsaM[a]	1	–
PsaX[a]	1	–
PG bound[b]	1	1
PsaH[c]	–	1
PsaG[c]	–	1
total	11	13
total PSI core	96	101
	Peripheral Chl *a*/*b*-Binding Antenna	
Lhca1	–	14
Lhca4	–	16
Lhca2	–	14
Lhca3	–	13
gap Chls	–	10
total LHCI	–	67
total	96	168

[a] Cyanobacterium-specific PSI subunits. [b] Chls ligated by phosphatidylglycerol (PG) in cyanobacterial PSI (Chl 11801 in 1JBO) and supposedly in eukaryotic PSI (Chl 11901 in 1QZV). [c] Eukaryote-specific subunits.

as between neighboring Lhca proteins result in formation of a cleft between the PSI surface and the LHCI layer. Strong transmembrane helix−helix interactions observed between Lhca1 and the PsaG subunits are thought to anchor the peripheral antenna to the PSI core. External interhelical loops and terminal regions of the protein subunits from both sides of the interacting domains further stabilize the modular structure.

Despite the overall similar structures of the core chlorophyll networks between cyanobacterial and eukaryotic PSI, the PSI−LHCI supercomplex has some differences mainly associated with the structural coupling of the LHCI antenna. Modifications include changes in the orientation of several peripherally located Chls as well as binding of new Chls both by the PsaB protein and by the peripheral subunits of the PSI core, including two eukaryote-specific PsaH and PsaG subunits. Structural coupling of the LHCI antenna resulted in binding of 56 Chls that are nearly equally bound to four LHCI proteins and 10 extra Chls (gap Chls), which are located in the cleft between the LHCI belt and the PSI core (Table 1 and Figure 6).

The general structural feature of LHCI, which is shared with LHCII, is that each of six Chl *a* molecules (a1−a6) bound to conserved pigment-binding sites in helices I and III is involved in interaction with a closely located pigment, resulting in formation of strongly interacting dimers (*53*, *106*) (Figure 7). The majority of the pigments in both complexes occupy similar positions; however, it seems that the orientations of some of them are significantly different. This is a result of adjustment of the LHCI pigment orientations relative to the PSI core antenna. The changes also involve the apparent binding of extra pigments, including linkers in LHCI monomers and gap pigments in the cleft between the PSI core and LHCI. These pigments add to the structural connectivity of the peripheral antenna and the PSI core antenna network. Distribution of the gap pigments in the cleft is very uneven with seven of 10 pigments located near the interface between the Lhca1−Lhca4 heterodimer and the PSI core (Figure 6).

Low-Resolution Structural Models of the PSI−LHCI Supercomplex in State 1 and State 2. Recent single-particle electron microscopy studies of the PSI−LHCI supercomplex from *C. reinhardtii* (*14*, *16*, *116*), spinach (*13*), and *Arabidopsis thaliana* (*117*) confirmed the similar overall architecture of the eukaryotic PSI featuring Lhca proteins interacting predominantly with PsaA, PsaK, PsaF/PsaJ, PsaG, and PsaB surfaces of the PSI core.

In contrast to the 4.4 Å resolution crystal structure of the PSI−LHCI supercomplex from pea (Figure 6), the projection maps of the PSI−LHCI particles from *C. reinhardtii* visualized additional electron densities suggesting a larger peripheral antenna size in green algae PSI associated with the functional changes in antenna size (Figure 8A,B). Three low-resolution structural models of the PSI−LHCI supercomplexes have been reported (*14*, *16*, *116*). Kargul and colleagues have related their structures to state 1 (*16*) or state 2 (*116*) associated with excitation energy redistribution between PSI and PSII (*118*−*121*). In the structural model of PSI in state 2 (*116*) (Figure 8B), some of the monomeric LHC proteins were bound not only to the surface of the PSI subunits interacting with the LHCI belt but also to the surface in the vicinity of the PsaH subunit that was suggested to be a docking site for LHCII in response to state 1−state 2 transitions (*121*). Association of LHCII with PSI is thought to increase the antenna cross section in PSI at the expense of PSII (*119*, *122*).

Biochemical and structural analysis of the PSI−LHCI complex isolated from *C. reinhardtii* in state 2 (*116*) indicated that the extra density located close to PsaH was due to tightly bound phosphorylated CP29, an LHC-like protein normally associated with only PSII (Figure 9A). The authors suggest that this bound phospho-CP29 possibly provides a linker for the association of LHCII with PSI in state 2. Moreover, in light of the X-ray structure of the higher-plant PSI−LHCI supercomplex and taking into account estimates of areas of negative staining and detergent shell, Kargul et al. (*116*) concluded that the isolated state 1 PSI−LHCI supercomplex has six LHC proteins (Figure 8A), not 11 as previously suggested (*16*). In addition to four Lhca proteins along the PsaA, PsaK, PsaF/J, and PsaB surface, two monomeric LHC proteins are suggested to bind in the vicinity of PsaH and the phospho-CP29 binding site. Surprisingly, in higher plants, the structure of the PSI supercomplex in state 2 was found to be different. Kouřil et al. (*117*) identified structural association of the PSI−LHCI supercomplex and an LHCII trimer from *Ar. thaliana* as a pear-shaped PSI−LHCI−LHCII particle with the LHCII trimer docked to PsaH, PsaL, PsaA, and PsaK surfaces of the PSI core (Figure 9B). The authors have not ruled out a possibility of the second LHCII trimer-docking site in the symmetry-related position covered by the PsaH, PsaI, PsaB, and PsaG subunits.

Structural differences in the PSI supercomplexes observed under state 2 conditions in green algae and higher plants

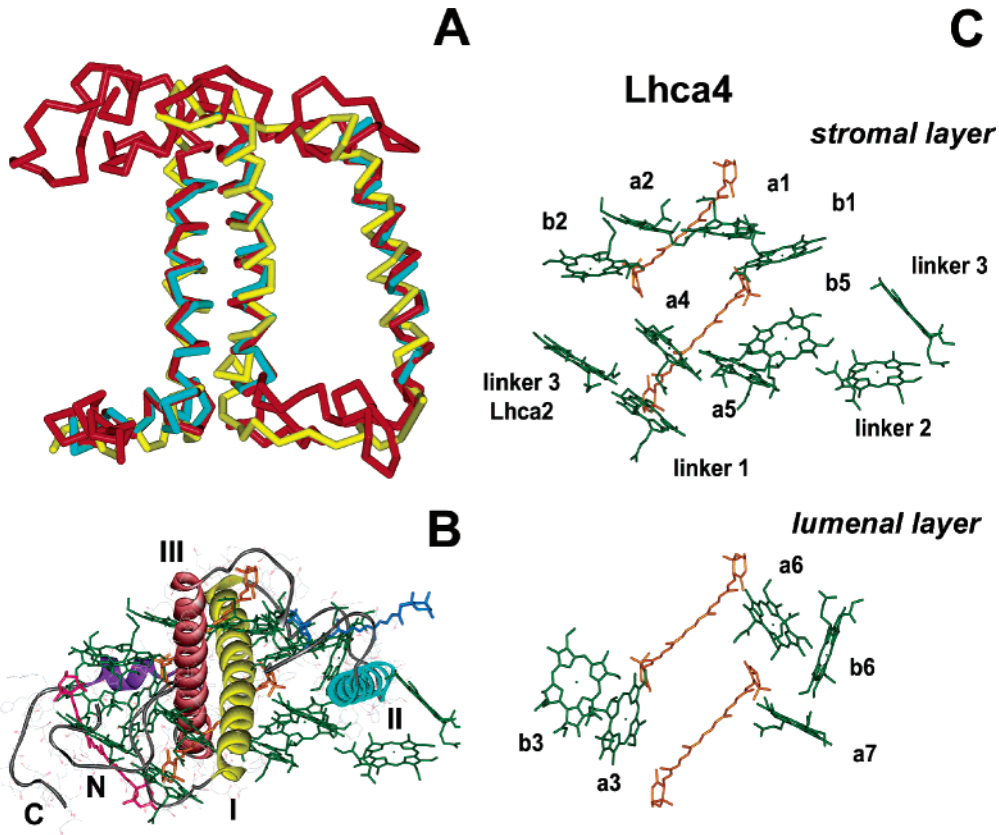

FIGURE 7: Structure of the Chl *a*/*b*-binding light-harvesting complex from the peripheral LHCI antenna of photosystem I. (A) Overlap of the α-carbon traces of LHCII from spinach [red, PDB entry 1RWT (*106*)], LHCII from pea [blue, atomic coordinates courtesy of W. Kühlbrandt (*105*)], and Lhca4 from the PSI−LHCI supercomplex from pea [yellow, PDB entry 1QZV (*15*)]. (B) Top view of the three-dimensional model of the Lhca4 polypeptide based on secondary structure prediction and structural homologies of LHCI and LHCII (*53*, *107*). N and C label the N- and C-termini, respectively. I−IV are the transmembrane helices. (C) Stromal (top panel) and lumenal (bottom panel) layers of pigments in Lhca4. For the sake of comparison, the majority of pigments are labeled according to the method of Kühlbrandt et al. (*105*). Linker pigments are labeled according to the method of Ben-Shem et al. (*15*).

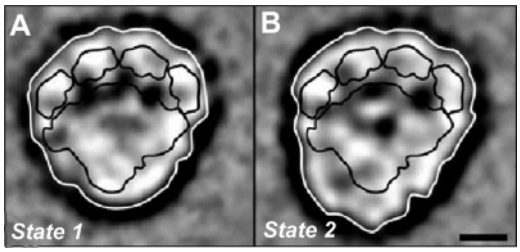

FIGURE 8: Structure of the PSI−LHCI supercomplexes from the green alga *C. reinhardtii* in different functional states. (A) Top-view projection of an electron microscopy image of the PSI−LHCI supercomplex in state 1. (B) Complex in state 2. The projections are overlaid with outlines of the X-ray structural model of the PSI−LHCI supercomplex from pea (PDB entry 1QZV). The scale bar is 50 Å. Reprinted with permission from ref *116*. Copyright 2005 Blackwell.

indicate either differences in structural coupling of LHC proteins and the PSI core or species-dependent functional differences in regulatory state 2.

Functioning of the PSI−LHCI Supercomplex. The main functions of the peripheral LHCI antenna in the PSI−LHCI supercomplex from photosynthetic eukaryotes are accessory light harvesting and efficient delivery of the excitation to the PSI core complex before its dissipation or conversion into the long-lived triplet states giving rise to the deleterious singlet oxygen species. Mechanisms of the delivery of the excitation energy from the LHCI peripheral antenna to the PSI core in the PSI−LHCI supercomplexes from green algae and higher plants are poorly understood. For a long time, analyses of the energy transfer processes in the PSI−LHCI supercomplex from green algae and higher plants were complicated by kinetic heterogeneity associated with variability in lifetimes of excitation energy transfer processes and the photochemical trapping (reviewed in ref *28*). Since the excitation dynamics in eukaryotic and cyanobacterial PSI core antennas are largely similar (see above), such a heterogeneity was suggested to originate from a specific energy coupling of LHCI to the PSI core (*46*, *59*).

(1) Energy Transfer in LHCI Monomers and Dimers. Binding of Chl *b*, Chl *a*, and carotenoids by LHCI provides an additional increase in the absorption cross section of the PSI reaction center. Time-resolved studies revealed that excitation of Chl *b* in Lhca1 or Lhca4 rapidly populates the main Chl *a* spectral forms within 0.3−0.7 ps (*123*−*127*). This sub-picosecond energy transfer process corresponds to energy redistribution among the neighboring pigments within the stromal or lumenal layers of the LHCI monomer. Within each layer, the excitation energy flow is directed from peripherally located pigments (usually Chl *b*) toward Chl *a* molecules bound to conserved pigment binding sites of transmembrane helix I or III (Figure 7).

Each Chl *a* in this group approaches a carotenoid molecule (lutein) at a distance of 4−5 Å. This contact establishes another energy transfer pathway in LHCI, which is remarkably able to function in both directions. It enables transfer of the excitation energy from carotenoids to central Chl *a* molecules

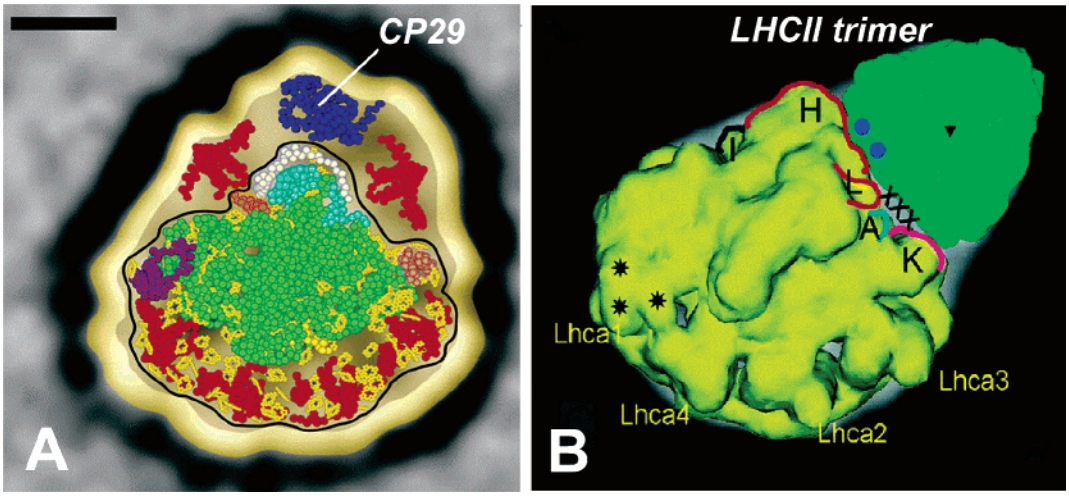

FIGURE 9: Comparison of structural models of PSI−LHCI supercomplexes in state 2 from green algae (A) and higher plants (B). The projection map for the state 2 PSI−LHCI supercomplex from *C. reinhardtii* is modeled using higher plant coordinates from 1qzv (*15*) with the PSI core (green), the LHCI antenna (red), and the PsaJ (yellow), PsaK (magenta), PsaG (purple), PsaI (orange), PsaL (cyan), and PsaH (white) subunits. The additional density observed in the state 2 PSI−LHCI supercomplex, which is able to accommodate an additional LHC subunit, is colored blue and is suggested to be phospho-CP29. Panel A is modified from ref *116*. (B) Projection map of the state 2 PSI−LHCI−LHCII supercomplex from *Ar. thaliana* fitted with high-resolution structures of PSI (yellow; *15*) and trimeric LHCII (green; *106*). Panel B reprinted with permission from ref *117*. Copyright 2005 American Chemical Society.

within ~100 fs via the S_2−Q_y channel (*126*, *127*). In a reverse direction (Chl *a* to carotenoids), this pathway would supposedly work as a photoprotective valve enabling either quenching of the Chl excitation via direct electron charge exchange between Chl *a* and the carotenoid molecule (*128*, *129*) or quenching of unused (or undelivered) excitation in the form of Chl *a* triplet states by carotenoids that prevents formation of toxic singlet oxygen (*105*).

Within 3−5 ps, the excitation was shown to be redistributed among the major Chl *a* forms in both lumenal and stromal pigment layers with significant localization of the excitation on the low-energy absorbing pigments (red pigments) in the 680−710 nm spectral region (*123*−*125*). In all Lhca proteins uncoupled from the PSI core, the red pigments serve as terminal emitters characterized by a significant red shift of the fluorescence (20−50 nm) (*130*−*135*). The extent of the red shift in different Lhca proteins is thought to be determined by the specific molecular environment of pigment cluster a5−b5 in the helix I−helix II interface (*53*, *107*, *134*−*137*) (Figure 7). In LHCII trimers, the terminal emitter is located in a different place and involves different pigments (*106*).

In vitro, Lhca proteins tend to form dimers (*108*). In Lhca1−Lhca4 heterodimers that are characterized by assembly of extra Chl *b* molecules (*130*, *131*), time-resolved absorption (*123*) and fluorescence spectroscopy studies (*126*, *138*) revealed an extra energy transfer component with lifetimes varying in the range of 15−30 ps. This energy transfer process was ascribed to intersubunit energy redistribution within the LHCI dimers, specifically in Lhca1−Lhca4 heterodimers (*138*). Similar processes were shown to occur in LHCII trimers (*139*).

The slow intersubunit energy equilibration in the Lhca1−Lhca4 heterodimer might be explained by a large distance (~40 Å) between a5−b5 of the energy donor and a5−b5 of the energy acceptor, at least between Lhca1 and Lhca4 (Figure 10). Furthermore, the presence of Chl *b* between Lhca subunits in the LHCI belt could be a cause of this slow energy transfer process due to the fact that Chl *b* is higher

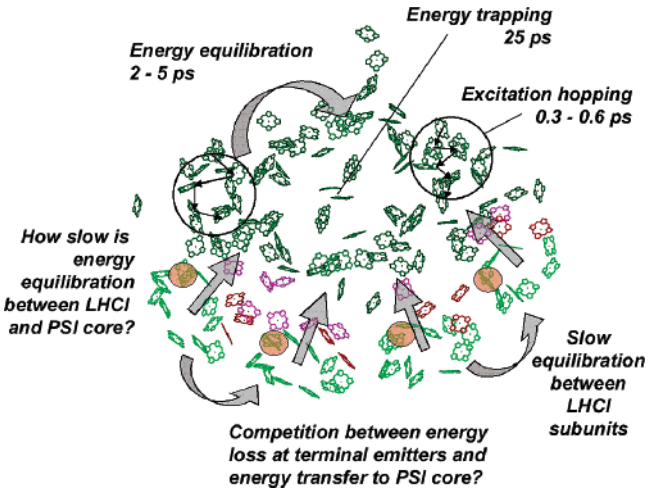

FIGURE 10: Functional organization of the PSI−LHCI supercomplexes from higher plants. Excitation dynamics in the PSI monomer is similar to that in cyanobacteria (see Figure 3). The cause of slow excitation equilibration (70−100 ps) between LHCI and the PSI core is suggested to arise either from slow energy equilibration between Lhca subunits or from competition between energy losses in LHCI and energy transfer to PSI. The color code for Chls follows: dark green for PSI core Chls, light green for LHCI Chls, red for linkers between LHCI, and magenta for gap pigments. Shaded circles show locations of terminal emitters in LHCI. See the text for details.

in energy than Chl *a*. The crystal structure of LHCII (*106*) demonstrates that Chl *b* molecules are located largely in the intersubunit interface due to a peripheral binding of Chl *b* within each subunit. If a similar situation occurs in the LHCI dimers, it might affect the excitation dynamics in the PSI−LHCI supercomplex (see below).

(2) Energy Transfer from LHCI to the PSI Core. Time-resolved spectroscopy studies of the PSI−LHCI supercomplex from green algae and higher plants show a biphasic overall decay of the excitation consisting of 20−50 ps photochemical trapping in the PSI core antenna (see section I) and the slower excitation trapping phase with the lifetime varying in the range of 70−150 ps (*46*, *140*−*142*). It is

puzzling that the experimentally observed slower excitation energy decay in the PSI−LHCI supercomplex is associated with Chl *a*/*b* binding peripheral LHCI antenna since the presence of the gap pigments between LHCI and the PSI provides structural connectivity that would enable fast energy equilibration between the periphery and the core antenna (*15*). Indeed, kinetic modeling based on the crystal structure of the PSI from higher plants (*56*) predicted an overall excitation lifetime of the PSI−LHCI network of 49 ps and computed excitation energy transfer times from LHCI to the PSI core via unevenly distributed gap pigments (see Figures 6 and 10) in the range from 1.5 ps for the Lhca1−Lhca4 form, 2.5 ps for Lhca3, and 6 ps for Lhca2. The experimentally observed slower excitation equilibration between LHCI and the PSI core is in contrast to excitation dynamics in the PSI−CP43′ supercomplexes from cyanobacteria with excitation equilibration of the peripheral antenna and the PSI core antenna occurring long before the photochemical trapping in the PSI RC (*59*; see section II and Figure 5). The origin of the observed slow energy equilibration between the LHCI peripheral antenna and the PSI core is under debate.

Recently, Ihalainen et al. (*141*) have found a difference in the slow energy trapping time in the PSI−LHCI supercomplex from *Ar. thaliana* (83 ps) and *C. reinhardtii* (68 ps). The slower trapping phase in the PSI−LHCI supercomplex from higher plants was interpreted as an effect of a larger amount of red pigments in LHCI from higher plants even though the functional antenna size in the PSI−LHCI supercomplex from green algae seems to be bigger as visualized by recent low-resolution electron microscopy studies (*14*, *16*, *116*). Red pigments in LHCI are involved in localization of the excitation on terminal emitters (see above). Chl clusters forming terminal emitters of LHCI (largely in Lhca3 and Lhca4) were suggested to slow energy equilibration between LHCI and PSI through competition between the LHCI-to-PSI energy transfer channel and the energy loss channel in the terminal emitter (*53*, *142*) (see Figure 10). At low temperatures, the red pigments in LHCI act as deep excitation traps, resulting in a possible functional uncoupling of LHCI from the PSI core (*142*). The energy losses in terminal emitters might result in the observed variation of the lifetime (80−120 ps) of the slow energy excitation decay in the PSI−LHCI supercomplex from *C. reinhardtii* (*46*, *142*).

Kinetic evidence of possible energy losses in the peripheral antenna at physiological temperatures is associated with detection of excitation decay processes in isolated LHCI dimers with lifetimes ranging from tens of picoseconds to several hundred picoseconds (*53*, *126*, *127*, *138*, *140*, *141*). Recent target analysis of the time-resolved fluorescence of the PSI−LHCI supercomplex from *Ar. thaliana* and *C. reinhardtii* (*141*) suggested that these excitation energy decay processes might be a cause of the decrease to ∼80% of the photochemical trapping yield in the PSI−LHCI supercomplex as compared to the ∼95% yield in the PSI−LHCI supercomplex calculated in the crystal structure-based kinetic modeling (*56*). Energy dissipation of chlorophyll clusters in LHCI is likely to be related to photoprotection against excess energy, although this has not been experimentally established. Recently reported increased levels of de-epoxidation of violaxanthins in Lhca3 and Lhca4 (*143*) indicate the possible involvement of carotenoids in the process.

Structural changes of the LHCI peripheral antenna in response to changed environmental conditions (*144*) are among the factors, although far less studied, influencing the efficiency of the energy transfer from LHCI to the PSI core. Iron stress of green algae was shown to result in an impairment of the excitation energy transfer in the peripheral antenna associated with N-terminal processing of Lhca3 (*145*). A specific Lhca5 subunit of LHCI in PSI from higher plants (*146*−*148*) was suggested to interact with Lhca2 or Lhca3 under high-light intensity conditions. A 120 ps component of energy trapping in the PSI−LHCI supercomplex from *Arabidopsis* mutants depleted of the majority of Lhca proteins was associated with functioning of this LHCI subunit (*149*).

The kinetic consequences of binding of LHCII to the PSI−LHCI supercomplex under state 2 conditions (see Figures 8 and 9) are unknown. Additional Chls observed in the eukaryotic PSI core in the region adjacent to PsaL and PsaH are likely to provide functional connectivity of Chls in LHCII complexes docked to the PSI core with a cluster of red pigments associated with the linker Chl (B37−B38). It is interesting to suggest whether this pigment cluster could participate in downhill enhancement of energy transfer from LHCII to the PSI core (*53*).

In conclusion, the functional connectivity of LHCI and PSI via gap pigments and the relative location of the terminal emitters in Lhca proteins might play an important role in determining the dynamic ratio between the direct energy transfer from largely isoenergetic peripheral antenna and the PSI core and possible energy losses in the peripheral antenna. Energy coupling in the eukaryotic PSI−LHCI supercomplexes is probably a result of the structural adaptation of the LHCI peripheral antenna that not only extends the absorption cross section of the PSI core but also participates in regulation of excitation flows between the two photosystems as well as in photoprotection.

REFERENCES

1. Blankenship, R. E. (2002) *Molecular Mechanisms of Photosynthesis*, Blackwell Science, Oxford, U.K.
2. Barber, J. (2003) Photosystem II: The engine of life, *Q. Rev. Biophys. 36*, 71−89.
3. Chitnis, P. R. (2001) Photosystem I: Function and physiology, *Annu. Rev. Plant Physiol. Plant Mol. Biol. 52*, 593−626.
4. Golbeck, J. H. (2003) The binding of cofactors to photosystem I analyzed by spectroscopic and mutagenic methods, *Annu. Rev. Biophys. Biomol. Struct. 32*, 237−256.
5. Schubert, W. D., Klukas, O., Saenger, W., Witt, H. T., Fromme, P., and Krauss, N. (1998) A common ancestor for oxygenic and anoxygenic photosynthetic systems: A comparison based on the structural model of photosystem I, *J. Mol. Biol. 280*, 297−314.
6. Jordan, P., Fromme, P., Witt, H. T., Klukas, O., Saenger, W., and Krauss, N. (2001) Three-dimensional structure of cyanobacterial photosystem I at 2.5 Å resolution, *Nature 411*, 909−917.
7. Melkozernov, A. N., and Blankenship, R. E. (2006) Photosynthetic functions of chlorophylls, in *Chlorophylls and Bacteriochlorophylls: Biochemistry, Biophysics and Biological Function* (Grimm, B., Porra, R. J., Rüdiger, W., and Scheer, H., Eds) Kluwer Academic Publishers, Dordrecht, The Netherlands (in press).
8. Asada, K. (1999) The water−water cycle in chloroplasts: Scavenging of active oxygens and dissipation of excess photons, *Annu. Rev. Plant Physiol. Plant Mol. Biol. 50*, 601−639.
9. Grossman, A. R., Bhaya, D., and He, Q. (2001) Tracking the light environment by cyanobacteria and the dynamic nature of light harvesting, *J. Biol. Chem. 276*, 11449−11452.
10. Gantt, E., Grabowski, B., and Cunningham, F. X., Jr. (2003) Antenna systems in red algae: Phycobilisomes with photosystem II and chlorophyll complexes with photosystem I, in *Light-har-*

vesting antennas (Green, B. R., and Parson, W. W., Eds.) pp 307−322, Kluwer Academic Publishers, Dordrecht, The Netherlands.
11. Bibby, T. S., Nield, J., and Barber, J. (2001) Iron deficiency induces the formation of an antenna ring around trimeric photosystem I in cyanobacteria, *Nature 412*, 743−745.
12. Boekema, E. J., Hifney, A., Yakushevska, A. E., Piotrowski, M., Keegstra, W., Berry, S., Michel, K. P., Pistorius, E. K., and Kruip, J. (2001) A giant chlorophyll-protein complex induced by iron deficiency in cyanobacteria, *Nature 412*, 745−748.
13. Boekema, E. J., Jensen, P. E., Schlodder, E., van Breemen, J. F. L., van Roon, H., Scheller, H. V., and Dekker, J. P. (2001) Green plant Photosystem I binds light-harvesting complex I on one side of the complex, *Biochemistry 40*, 1029−1036.
14. Germano, M., Yakushevska, A. E., Keegstra, W., van Gorkom, H. J., Dekker, J. P., and Boekema, E. J. (2002) Supramolecular organization of photosystem I and light-harvesting complex I in *Chlamydomonas reinhardtii*, *FEBS Lett. 525*, 121−125.
15. Ben-Shem, A., Frolow, F., and Nelson, N. (2003) Crystal structure of plant photosystem I, *Nature 426*, 630−635.
16. Kargul, J., Nield, J., and Barber, J. (2003) Three-dimensional reconstruction of a light-harvesting complex I-photosystem I (LHCI−PSI) supercomplex from the green alga *Chlamydomonas reinhardtii*: Insights into light harvesting for PSI, *J. Biol. Chem. 278*, 16135−16141.
17. Dekker, J. P., and Boekema, E. J. (2005). Supramolecular organization of thylakoid membrane proteins in green plants, *Biochim. Biophys. Acta 1706*, 12−39.
18. Melkozernov, A. N., Lin, S., and Blankenship, R. E. (2000) Excitation dynamics and heterogeneity of energy equilibration in the core antenna of Photosystem I from the cyanobacterium *Synechocystis* sp. PCC 6803, *Biochemistry 39*, 1489−1498.
19. Byrdin, M., Jordan, P., Krauss, N., Fromme, P., Stehlik, D., and Schlodder, E. (2002) Light harvesting in Photosystem I: Modeling based on the 2.5-Å structure of Photosystem I from *Synechococcus* elongatus, *Biophys. J. 83*, 433−457.
20. Chitnis, V. P., and Chitnis, P. R. (1993) PsaL subunit is required for the formation of photosystem I trimers in the cyanobacterium *Synechocystis sp*. PCC 6803, *FEBS Lett. 336*, 330−334.
21. Schluchter, W. M., Shen, G., Zhao, J., and Bryant, D. A. (1996) Characterization of PsaI and PsaL mutants of *Synechococcus sp*. strain PCC 7002: A new model for state transitions in cyanobacteria, *Photochem. Photobiol. 64*, 53−66.
22. Loll, B., Raszewski, G., Saenger, W., and Biesiadka, J. (2003) Functional role of Cα−H···O hydrogen bonds between transmembrane α-helices in Photosystem I, *J. Mol. Biol. 328*, 737−747.
23. Kruip, J., Bald, D., Boekema, E., and Rögner, M. (1994) Evidence for the existence of trimeric and monomeric photosystem-I complexes in thylakoid membranes from cyanobacteria, *Photosynth. Res. 40*, 279−286.
24. Kruip, J., Karapetyan, N. V., Terekhova, I. V., and Rögner, M. (1999) In vitro oligomerization of a membrane protein complex. Liposome-based reconstitution of trimeric photosystem I from isolated monomers, *J. Biol. Chem. 274*, 18181−18188.
25. Xu, Q., Hioppe, D., Chitnis, V. P., Odom, W. R., Guikema, J. A., and Chitnis, P. R. (1995) Mutational analysis of photosystem-I polypeptides in the cyanobacterium *Synechocystis sp*. PCC-6803: Targeted inactivation of PsaI reveals the function of PsaI in the structural organization of PsaL, *J. Biol. Chem. 270*, 16243−16250.
26. Kruip, J., Chitnis, P. R., Lagoutte, B., Rögner, M., and Boekema, E. J. (1997) Structural organization of the major subunits in cyanobacterial photosystem 1: Localization of subunits PsaC, -D, -E, -F, and -J, *J. Biol. Chem. 272*, 17061−17069.
27. Şener, M. K., Park, S., Lu, D. Y., Damjanović, A., Ritz, T., Fromme, P., and Schulten, K. (2004) Excitation migration in trimeric cyanobacterial photosystem I, *J. Chem. Phys. 120*, 11183−11195.
28. Van Grondelle, R., Dekker, J. P., Gillbro, T., and Sundström, V. (1994) Energy transfer and trapping in photosynthesis, *Biochim. Biophys. Acta 1187*, 1−65.
29. Fleming, G. R., and van Grondelle, R. (1997) Femtosecond spectroscopy of photosynthetic light-harvesting systems, *Curr. Opin. Struct. Biol. 7*, 738−748.
30. Gobets, B., and van Grondelle, R. (2001) Energy transfer and trapping in photosystem I, *Biochim. Biophys. Acta 1507*, 80−99.
31. Melkozernov, A. N. (2001) Excitation energy transfer in Photosystem I from oxygenic organisms, *Photosynth. Res. 70*, 129−153.
32. Melkozernov, A. N., Lin, S., and Blankenship, R. E. (2000) Femtosecond transient spectroscopy and excitonic interactions in Photosystem I, *J. Phys. Chem. B 104*, 1651−1656.
33. Melkozernov, A. N., Lin, S., Blankenship, R. E., and Valkunas, L. (2001) Spectral inhomogeneity of Photosystem I and its influence on excitation equilibration and trapping in *Synechocystis sp.* PCC 6803 at 77 K, *Biophys. J. 81*, 1144−1154.
34. Savikhin, S., Xu, W., Soukoulis, V., Chitnis, P. R., and Struve, W. (1999) Ultrafast primary processes in photosystem I of the cyanobacterium *Synechocystis sp.* PCC 6803, *Biophys. J. 76*, 3278−3288.
35. Gobets, B., van Stokkum, I. H., Rögner, M., Kruip, J., Schlodder, E., Karapetyan, N. V., Dekker, J. P., van Grondelle, R. (2001) Time-resolved fluorescence emission measurements of photosystem I particles of various cyanobacteria: A unified compartmental model, *Biophys. J. 81*, 407−424.
36. Kennis, J. T. M., Gobets, B., van Stokkum, I. H. M., Dekker, J. P., van Grondelle, R., and Fleming, G. R. (2001) Light-harvesting by chlorophylls and carotenoids in the photosystem I core complex of *Synechococcus elongatus*. A fluorescence upconversion study, *J. Phys. Chem. B 105*, 4485−4494.
37. De Weerd, F. L., Kennis, J. T. M., Dekker, J. P., and van Grondelle, R. (2003) β-Carotene to chlorophyll singlet energy transfer in the Photosystem I core of *Synechococcus elongatus* proceeds via the β-carotene S_2 and S_1 states, *J. Phys. Chem. B 107*, 5995−6002.
38. Polivka, T., and Sundström, V. (2004) Ultrafast dynamics of carotenoid excited states-from solution to natural and artificial systems, *Chem. Rev. 104*, 2021−2071.
39. Hastings, G., Kleinherenbrink, A. M., Lin, S., and Blankenship, R. E. (1994) Time-resolved fluorescence and absorption spectroscopy of photosystem I, *Biochemistry 33*, 3185−3192.
40. Hastings, G., Reed, L. J., Lin, S., and Blankenship, R. E. (1995) Excited-state dynamics in photosystem I: Effects of detergent and excitation wavelength, *Biophys. J. 69*, 2044−2055.
41. Hastings, G., Hoshina, S., Webber, A. N., and Blankenship, R. E. (1995) Universality of energy and electron-transfer processes in photosystem I, *Biochemistry 34*, 15512−15522.
42. Melkozernov, A. N., Su, H., Lin, S., Bingham, S., Webber, A. N., and Blankenship, R. E. (1997) Specific mutation near the primary donor in photosystem I from *Chlamydomonas reinhardtii* alters the trapping time and spectroscopic properties of P_{700}, *Biochemistry 36*, 2898−2907.
43. Gobets, B., van Stokkum, I. H. M., van Mourik, F., Dekker, J. P., and van Grondelle, R. (2003) Excitation wavelength dependence of the fluorescence kinetics in Photosystem I particles from *Synechocystis* PCC 6803 and *Synechococcus elongatus*, *Biophys. J. 85*, 3883−3898.
44. Du, M., Xie, X., Jia, Y. W., Mets, L., and Fleming, G. R. (1993) Direct observation of ultrafast energy-transfer in PS I core antenna, *Chem. Phys. Lett. 201*, 536−542.
45. White, N. T. H., Beddard, G. S., Thorne, J. R. G., Feehan, T. M., Keyes, T. E., and Heathcote, P. (1996) Primary charge separation and energy transfer in the photosystem I reaction center of higher plants, *J. Phys. Chem. 100*, 12086−12099.
46. Melkozernov, A. N., Kargul, J., Lin, S., Barber, J., and Blankenship, R. E. (2004) Energy coupling in the PSI-LHCI supercomplex from the green alga *Chlamydomonas reinhardtii*, *J. Phys. Chem. B 108*, 10547−10555.
47. Gibasiewicz, K., Ramesh, V. M., Melkozernov, A. N., Lin, S., Woodbury, N. W., Blankenship, R. E., and Webber, A. N. (2001) Excitation dynamics in the core antenna of PS I from *Chlamydomonas reinhardtii* CC2696 at room temperature, *J. Phys. Chem. B 105*, 11498−11506.
48. Yang, M., Damjanović, A., Vaswani, H. M., and Fleming, G. R. (2003) Energy transfer in photosystem I of cyanobacteria *Synechococcus elongatus*: Model study with structure-based semi-empirical Hamiltonian and experimental spectral density, *Biophys. J. 85*, 140−158.
49. Şener, M. K., Lu, D., Ritz, T., Park, S., Fromme, P., and Schulten, K. (2002) Robustness and optimality of light harvesting in cyanobacterial Photosystem I, *J. Phys. Chem. B 106*, 7948−7960.
50. Bruggemann, B., Sznee, K., Novoderezhkin, V., van Grondelle, R., and May, V. (2004) From structure to dynamics: Modeling exciton dynamics in the photosynthetic antenna PS1, *J. Phys. Chem. B 108*, 13536−13546.
51. Damjanovic, A., Vaswani, H. M., Fromme, P., and Fleming, G. R. (2002) Chlorophyll excitations in photosystem I of *Synechococcus elongatus*, *J. Phys. Chem. B 106*, 10251−10262.

52. Trissl, H.-W. (1993) Long-wavelength absorbing antenna pigments and heterogeneous absorption bands concentrate excitons and increase absorption cross section, *Photosynth. Res. 35*, 247−263.
53. Melkozernov, A. N., and Blankenship, R. E. (2005) Structural and functional organization of the peripheral light-harvesting system in Photosystem I, *Photosynth. Res. 85*, 33−50.
54. Savikhin, S., Xu, W., Chitnis, P. R., and Struve, W. (2000) Ultrafast primary processes in PS I from *Synechocystis sp.* PCC 6803: Roles of P_{700} and A_0, *Biophys. J. 79*, 1573−1586.
55. Müller, M. G., Niklas, J., Lubitz, W., and Holzwarth, A. R. (2003) Ultrafast transient absorption studies on Photosystem I reaction centers from *Chlamydomonas reinhardtii*. 1. A new interpretation of the energy trapping and early electron-transfer steps in Photosystem I, *Biophys. J. 85*, 3899−3922.
56. Şener, M., Jolley, C., Ben-Shem, A., Fromme, P., Nelson, N., Croce, R., and Schulten, K. (2005) Comparison of the light harvesting networks of plant and cyanobacterial photosystem I, *Biophys. J. 89*, 1630−1642.
57. Soukoulis, V., Savikhin, S., Xu, W., Chitnis, P. R., and Struve, W. (1999) Electronic spectra of PS I mutants: The peripheral subunits do not bind red chlorophylls in *Synechocystis sp.* PCC 6803, *Biophys. J. 76*, 2711−2715.
58. Turconi, S., Kruip, J., Schweitzer, G., Rögner, M., and Holzwarth, A. R. (1996) A comparative fluorescence kinetics study of Photosystem I monomers and trimers from *Synechocystis sp.* PCC 6803, *Photosynth. Res. 49*, 263−268.
59. Melkozernov, A. N., Bibby, T. S., Lin, S., Barber, J., and Blankenship, R. E. (2003) Time-resolved absorption and emission show that the CP43′ antenna ring of iron-stressed *Synechocystis sp* PCC6803 is efficiently coupled to the photosystem I reaction center core, *Biochemistry 42*, 3893−3903.
60. Pålsson, L.-O., Flemming, C., Gobets, B., van Grondelle, R., Dekker, J. P., and Schlodder, E. (1998) Energy transfer and charge separation in Photosystem I: P_{700} oxidation upon selective excitation of the long-wavelength antenna chlorophylls of *Synechococcus elongatus*, *Biophys. J. 74*, 2611−2622.
61. Karapetyan, N. V., Holzwarth, A. R., and Rögner, M. (1999) The photosystem I trimer of cyanobacteria: Molecular organization, excitation dynamics and physiological significance, *FEBS Lett. 460*, 395−400.
62. Schlodder, E., Cetin, M., Byrdin, M., Terekhova, I. V., and Karapetyan, N. V. (2005) $P700^+$- and $^3P700$-induced quenching of the fluorescence at 760 nm in trimeric Photosystem I complexes from the cyanobacterium *Arthrospira platensis*, *Biochim. Biophys. Acta 1706*, 53−67.
63. Karapetyan, N. V., Shubin, V. V., and Strasser, R. J. (1999) Energy exchange between the chlorophyll antenna of monomeric subunits within the Photosystem I trimeric complex of the cyanobacterium *Spirulina*, *Photosynth. Res. 61*, 291−301.
64. Owens, T. G., Webb, S. P., Alberte, R. S., Mets, L., and Fleming, G. R. (1988) Antenna structure and excitation dynamics in Photosystem-I. 1. Studies of detergent-isolated Photosystem-I preparations using time-resolved fluorescence analysis, *Biophys. J. 53*, 733−745.
65. Bibby, T. S., Nield, J., Partensky, F., and Barber, J. (2001) Oxyphotobacteria. Antenna ring around Photosystem I, *Nature 413*, 590.
66. Bibby, T. S., Mary, I., Nield, J., Partensky, F., and Barber, J. (2003) Low-light-adapted *Prochlorococcus* species possess specific antennae for each photosystem, *Nature 424*, 1051−1054.
67. Bumba, L., Prasil, O., and Vacha, F. (2005) Antenna ring around trimeric Photosystem I in chlorophyll *b* containing cyanobacterium *Prochlorothrix hollandica*, *Biochim. Biophys. Acta 1708*, 1−5.
68. Gantt, E. (1981) Phycobilisomes, *Annu. Rev. Plant Physiol. 32*, 327−347.
69. Glazer, A. N. (1982) Phycobilisomes: Structures and dynamics, *Annu. Rev. Microbiol. 36*, 173−198.
70. Martin, J. H., Coale, K. H., Johnson, K. S., Fitzwater, S. E., Gordon, R. M., Tanner, S. J., Hunter, C. N., Elrod, V. A., Nowicki, J. L., Coley, T. L., Barber, R. T., Lindley, S., Watson, A. J., Van Scoy, K., Law, C. S., Liddicoat, M. I., Ling, R., Stanton, T., Stockel, J., Collins, C., Anderson, A., Bidigare, R., Ondrusek, M., Latasa, M., Millero, F. J., Lee, K., Yao, W., Zhang, J. Z., Fredrich, G., Sakamoto, C., Chavez, F., Buck, K., Kolber, Z., Green, R., Falkowski, P. G., Chisholm, S. W., Hoge, F., Swift, R., Yungle, J., Turner, S., Nightingale, P., Hatton, A., Liss, P., and Tindale, N. W. (1994) Testing the iron hypothesis in ecosystems of the equatorial Pacific, *Nature 371*, 123−129.
71. Pakrasi, H. B., Riethman, H. C., and Sherman, L. A. (1985) Organization of pigment proteins in the Photosystem II complex of the cyanobacterium *Anacystis nidulans* R2, *Proc. Natl. Acad. Sci. U.S.A. 82*, 6903−6907.
72. Straus, N. A. (1994) Iron deprivation: Physiology and gene regulation, in *Molecular Biology of Cyanobacteria* (Bryant, D. A., Ed.) pp 731−750, Kluwer Academic Press, Dordrecht, The Netherlands.
73. Guikema, J., and Sherman, L. A. (1983) Organization and function of chlorophyll in membranes of cyanobacteria during iron starvation, *Plant Physiol. 73*, 250−256.
74. Laudenbach, D., and Strauss, N. A. (1988) Characterization of a cyanobacterial iron stress-induced gene similar to *psb*C, *J. Bacteriol. 170*, 5018−5026.
75. Burnap, R. L., Troyan, T., and Sherman, L. A. (1993) The highly abundant chlorophyll-protein of iron-deficient *Synechococcus* sp. PCC 7942 (CP43′) is encoded by the *isi*A gene, *Plant Physiol. 103*, 893−902.
76. Partensky, F., and Garczarek, L. (2003) The Photosynthetic Apparatus of Chlorophyll *b*- and *d*-containing Oxyphotobacteria, in *Photosynthesis: Photosynthesis in Algae* (Larkum, A. W., Douglas, S., and Raven, J. A., Eds.) pp 29−62, Kluwer Academic Publishers, Dordrecht, The Netherlands.
77. Ting, C. S., Rocap, G., King, J., and Chisholm, S. W. (2002) Cyanobacterial photosynthesis in the oceans: The origins and significance of divergent light-harvesting strategies, *Trends Microbiol. 10*, 134−142.
78. Michel, K. P., and Pistorius, E. K. (2004) Adaptation of the photosynthetic electron transport chain in cyanobacteria to iron deficiency: The function of *IdiA* and *IsiA*, *Physiol. Plant. 120*, 36−50.
79. Bibby, T. S., Nield, J., and Barber, J. (2001) Three-dimensional model and characterization of the iron stress-induced CP43′-photosystem I supercomplex isolated from the cyanobacterium *Synechocystis* PCC 6803, *J. Biol. Chem. 276*, 43246−43252.
80. Zouni, A., Witt, H.-T., Kern, J., Fromme, P., Krauss, N., Saenger, W., and Orth, P. (2001) Crystal structure of photosystem II from *Synechococcus elongatus* at 3.8 Å resolution, *Nature 409*, 739−743.
81. Nield, J., Morris, E. P., Bibby, T. S., and Barber, J. (2003) Structural analysis of the photosystem I supercomplex of cyanobacteria induced by iron deficiency, *Biochemistry 42*, 3180−3188.
82. Bibby, T. S., Nield, J., Chen, M., Larkum, A. W., and Barber, J. (2003) Structure of a photosystem II supercomplex isolated from *Prochloron didemni* retaining its chlorophyll *a/b* light-harvesting system, *Proc. Natl. Acad. Sci. U.S.A. 100*, 9050−9054.
83. Chen, M., Bibby, T. S., Nield, J., Larkum, A., and Barber, J. (2005) Iron deficiency induces a chlorophyll *d*-binding Pcb antenna system around Photosystem I in *Acaryochloris marina*, *Biochim. Biophys. Acta 1708*, 367−374.
84. Chen, M., Bibby, T. S., Nield, J., Larkum, A. W., and Barber, J. (2005) Structure of a large photosystem II supercomplex from *Acaryochloris marina*, *FEBS Lett. 579*, 1306−1310.
85. Bricker, T. M., and Frankel, L. K. (2002) The structure and function of CP47 and CP43 in photosystem II, *Photosynth. Res. 72*, 131−146.
86. Kamiya, N., and Shen, J.-R. (2003) Crystal structure of oxygen-evolving photosystem II from *Thermosynechococcus vulcanus* at 3.7 Å resolution, *Proc. Natl. Acad. Sci. U.S.A. 100*, 98−103.
87. Ferreira, K. N., Iverson, T. M., Maghlaoui, K., Barber, J., and Iwata, S. (2004) Architecture of the photosynthetic oxygen-evolving center, *Science 303*, 1831−1838.
88. Rhee, K. H., Morris, E. P., Barber, J., and Kühlbrandt, W. (1998) Three-dimensional structure of the plant photosystem II reaction centre at 8 angstrom resolution, *Nature 396*, 283−286.
89. Hankamer, B., Morris, E. P., and Barber, J. (1999) Revealing the structure of the oxygen-evolving core dimer of photosystem II by cryoelectron crystallography, *Nat. Struct. Biol. 6*, 560−564.
90. Vasil'ev, S., and Bruce, D. (2004) Optimization and evolution of light harvesting in photosynthesis: The role of antenna chlorophyll conserved between Photosystem II and Photosystem I, *Plant Cell 16*, 3059−3068.
91. Aspinwall, C. L., Duncan, J., Bibby, T., Mullineaux, C. W., and Barber, J. (2004) The trimeric organization of photosystem I is not necessary for the iron-stress induced CP43′ protein to functionally associate with this reaction center, *FEBS Lett. 574*, 126−130.
92. Kouřil, R., Arteni, A., Lax, J., Yeremenko, N., D'Haene, S., Rögner, M., Matthijs, H., Dekker, J., and Boekema E. (2005)

Structure and functional role of supercomplexes of IsiA and Photosystem I in cyanobacterial photosynthesis, *FEBS Lett. 579*, 3253−3257.
93. Andrizhiyevskaya, E. G., Schwabe, T. M., Germano, M., D'Haene, S., Kruip, J., van Grondelle, R., and Dekker, J. P. (2002) Spectroscopic properties of PSI−IsiA supercomplexes from the cyanobacterium *Synechococcus* PCC 7942, *Biochim. Biophys. Acta 1556*, 265−272.
94. Andrizhiyevskaya, E. G., Frolov, D., van Grondelle, R., and Dekker, J. P. (2004) Energy transfer and trapping in the Photosystem I complex of *Synechococcus* PCC 7942 and in its supercomplex with IsiA, *Biochim. Biophys. Acta 1656*, 104−113.
95. De Weerd, F. L., van Stokkum, I. H., van Amerongen, H., Dekker, J. P., and van Grondelle, R. (2002) Pathways for energy transfer in the core light-harvesting complexes CP43 and CP47 of photosystem II, *Biophys. J. 82*, 1586−1597.
96. Förster, Th. (1965) Delocalized Excitation and Excitation Transfer, in *Modern Quantum Chemistry* (Sinanoslu, O., Ed.) Part III, pp 93−137, Academic Press, New York.
97. Ihalainen, J. A., D'Haene, S., Yeremenko, N., van Roon, H., Arteni, A. A., Boekema, E. J., van Grondelle, R., Matthijs, H. C. P., and Dekker, J. P. (2005) Aggregates of the Chlorophyll-Binding Protein IsiA (CP43′) Dissipate Energy in Cyanobacteria, *Biochemistry 44*, 10846−10853.
98. Sarcina, M., and Mullineaux, C. W. (2004) Mobility of the IsiA chlorophyll-binding protein in cyanobacterial thylakoid membranes, *J. Biol. Chem. 279*, 36514−36518.
99. Scheller, H. V., Jensen, P. E., Haldrup, A., Lunde, C., and Knoetzel, J. (2001) Role of subunits in eukaryotic Photosystem I, *Biochim. Biophys. Acta 1507*, 41−60.
100. Jensen, P. E., Haldrup, A., Rosgaard, L., and Scheller, H. V. (2003) Molecular dissection of Photosystem I in higher plants: Topology, structure and function, *Physiol. Plant. 119*, 313−321.
101. Fromme, P., Melkozernov, A. N., Jordan, P., and Krauss, N. (2003) Structure and function of Photosystem I: Interaction with its soluble electron carriers and external antenna systems, *FEBS Lett. 555*, 40−44.
102. Khrouchtchova, A., Hansson, M., Paakkarinen, V., Vainonen, J. P., Zhang, S., Jensen, P. E., Scheller, H. V., Vener, A. V., Aro, E. M., and Haldrup, A. (2005) A previously found thylakoid membrane protein of 14 kDa (TMP14) is a novel subunit of plant photosystem I and is designated PSI-P, *FEBS Lett. 579*, 4808−4812.
103. Durnford, D. G., Deane, J. A., Tan, S., McFadden, G. I., Gantt, E., and Green, B. R. (1999) A phylogenetic assessment of the eukaryotic light-harvesting antenna proteins, with implications for plastid evolution, *J. Mol. Evol. 58*, 59−68.
104. Green, B. R. (2003) The Evolution of Light-harvesting Antennas, in *Light-harvesting antennas* (Green, B. R., and Parson, W. W., Eds.) pp 129−168, Kluwer Academic Publishers, Dordrecht, The Netherlands.
105. Kühlbrandt, W., Wang, D. N., and Fujiyoshi, Y. (1994) Atomic model of plant light-harvesting complex by electron crystallography, *Nature 367*, 614−621.
106. Liu, Z., Yan, H., Wang, K., Kuang, T., Zhang, J., Gui, L., An, X., and Chang, W. (2004) Crystal structure of spinach major light-harvesting complex at 2.72 Å resolution, *Nature 428*, 287−292.
107. Melkozernov, A. N., and Blankenship, R. E. (2003) Structural modeling of the Lhca4 subunit of LHCI-730 peripheral antenna in photosystem I based on similarity with LHCII, *J. Biol. Chem. 278*, 44542−44551.
108. Pichersky, I., and Jansson, S. (1996) The Light Harvesting Chlorophyll *a/b*-binding Polypeptides and Their Genes in Angiosperm and Gymnosperm Species, in *Oxygenic Photosynthesis: The Light Reactions* (Ort, D. R., and Yoccum, C. F., Eds.) pp 507−521, Kluwer Academic Publishers, Dordrecht, The Netherlands.
109. Jansson, S. (1999) A guide to the Lhc genes and their relatives in *Arabidopsis*, *Trends Plant Sci. 4*, 236−240.
110. Zolla, L., Rinalducci, S., Timperio, A. M., and Huber, C. G. (2002) Proteomics of light-harvesting proteins in different plant species. Analysis and comparison by liquid chromatography-electrospray ionization mass spectrometry. Photosystem I, *Plant Physiol. 130*, 1938−1950.
111. Hippler, M., Klein, J., Fink, T., Allinger, T., and Hoerth, P. (2001) Towards functional proteomics of membrane protein complexes: Analysis of thylakoid membrane fractions in *Chlamydomonas reinhardtii*, *Plant J. 28*, 595−606.
112. Stauber, E. J., Fink, A., Markert, C., Kruse, O., Johanningmeier, U., and Hippler, M. (2003) Proteomics of *Chlamydomonas reinhardtii* light-harvesting proteins, *Eukaryotic Cell 2*, 978−994.
113. Tokutsu, R., Teramoto, H., Takahashi, Y., Ono, T. A., and Minagawa, J. (2004) The light-harvesting complex of photosystem I in *Chlamydomonas reinhardtii*: Protein composition, gene structures and phylogenic implications, *Plant Cell Physiol. 45*, 138−145.
114. Elrad, D., and Grossman, A. R. (2004) A genome's-eye view of the light-harvesting polypeptides of *Chlamydomonas reinhardtii*, *Curr. Genet. 45*, 61−75.
115. Takahashi, Y., Yasui, T., Stauber, E. J., and Hippler, M. (2004) Comparison of the subunit compositions of the PSI-LHCI supercomplex and the LHCI in the green alga *Chlamydomonas reinhardtii*, *Biochemistry 43*, 7816−7823.
116. Kargul, J., Turkina, M. V., Nield, J., Benson, S., Vener, A. V., and Barber, J. (2005) Light-harvesting complex II protein CP29 binds to photosystem I of *Chlamydomonas reinhardt*ii under State 2 conditions, *FEBS Lett. 272*, 4797−4806.
117. Kouřil, R., Zygadlo, A., Arteni, A. A., de Wit, C. D., Dekker, J. P., Jensen, P. E., Scheller, H. V., and Boekema, E. J. (2005) Structural characterization of a complex of Photosystem I and Light-Harvesting Complex II of *Arabidopsis thaliana*, *Biochemistry 44*, 10935−10940.
118. Wollman, F.-A. (2001) State transitions reveal dynamics and flexibility of the photosynthetic apparatus, *EMBO J. 20*, 3623−3630.
119. Rochaix, J.-D. (2001) Assembly, function, and dynamics of the photosynthetic machinery in *Chlamydomonas reinhardtii*, *Plant Physiol. 127*, 1394−1398.
120. Allen, J. F. (2003) State transitions: A question of balance, *Science 299*, 1530−1532.
121. Lunde, C., Jensen, P. E., Haldrup, A., Knoetzel, J., and Scheller, H. V. (2000) The PSI−H subunit of Photosystem I is essential for state transitions in plant photosynthesis, *Nature 408*, 613−615.
122. Haldrup, A., Jensen, P. E., Lunde, C., and Scheller, H. V. (2002) Balance of power: A view of the mechanism of photosynthetic state transitions, *Trends Plant Sci. 6*, 301−305.
123. Melkozernov, A. N., Lin, S., Schmid, V., Paulsen, H., Schmidt, G. W., and Blankenship, R. E. (2000) Ultrafast excitation dynamics of low energy pigments in reconstituted peripheral light-harvesting complexes of photosystem I, *FEBS Lett. 471*, 89−92.
124. Melkozernov, A. N., Lin, S., Schmid, V. H. R., Lago-Places, E., Paulsen, H., and Blankenship, R. E. (2001) Molecular origin of red pigments in the peripheral light-harvesting antenna of Photosystem I: Ultrafast absorption spectroscopy of recombinant Lhca, in *Proceedings of the 12th International Congress on Photosynthesis*, CSIRO Publishing, Melbourne, Australia.
125. Melkozernov, A. N., Schmid, V. H. R., Lin, S., Paulsen, H., and Blankenship, R. E. (2002) Excitation energy transfer in the Lhca1 subunit of LHCI-730 peripheral antenna of photosystem I, *J. Phys. Chem. B 106*, 4313−4317.
126. Gobets, B., Kennis, J. T. M., Ihalainen, J. A., Brazzoli, M., Croce, R., van Stokkum, I. H. M., Bassi, R., Dekker, J., van Amerongen, H., Fleming, G. R., and van Grondelle, R. (2001) Excitation energy transfer in dimeric light-harvesting complex I: A combined streak-camera/fluorescence upconversion study, *J. Phys. Chem. B 105*, 10132−10139.
127. Gibasiewicz, K., Croce, R., Morosinotto, T., Ihalainen, J. A., van Stokkum, I. H., Dekker, J. P., Bassi, R., and van Grondelle, R. (2005) Excitation energy transfer pathways in Lhca4, *Biophys. J. 88*, 1959−1969.
128. Ma, Y. Z., Holt, N. E., Li, X. P., Niyogi, K. K., and Fleming, G. R. (2003) Evidence for direct carotenoid involvement in the regulation of photosynthetic light harvesting, *Proc. Natl. Acad. Sci. U.S.A. 100*, 4377−4382.
129. Holt, N. E., Zigmantas, D., Valkunas, L., Li, X. P., Niyogi, K. K., and Fleming, G. R. (2005) Carotenoid cation formation and the regulation of photosynthetic light harvesting, *Science 307*, 433−436.
130. Schmid, V. H. R., Cammarata, K. V., Bruns, B. U., and Schmidt, G. W. (1997) *In vitro* reconstitution of the photosystem I light-harvesting complex LHC I-730: Heterodimerization is required for antenna pigment organization, *Proc. Natl. Acad. Sci. U.S.A. 94*, 7667−7672.
131. Croce, R., Morosinotto, T., Castelletti, S., Breton, J., and Bassi, R. (2002) The Lhca antenna complexes of higher plants photosystem I, *Biochim. Biophys. Acta 1556*, 29−40.

132. Tjus, S. E., Roobol-Boza, M., Pålsson, L. O., and Andersson, B. (1995) Rapid isolation of Photosystem I chlorophyll-binding proteins by anion exchange perfusion chromatography, *Photosynth. Res. 45*, 41−49.
133. Ganeteg, U., Strand, A., Gustafsson, P., and Jansson, S. (2001) The properties of the chlorophyll *a/b*-binding proteins Lhca2 and Lhca3 studied in vivo using antisense inhibition, *Plant Physiol. 127*, 150−158.
134. Castelletti, S., Morosinotto, T., Robert, B., Caffarri, S., Bassi, R., and Croce, R. (2003) Recombinant Lhca2 and Lhca3 subunits of the Photosystem I antenna system, *Biochemistry 42*, 4226−4234.
135. Morosinotto, T., Castelletti, S., Breton, J., Bassi, R., and Croce, R. (2002) Mutation analysis of Lhca1 antenna complex. Low energy absorption forms originate from pigment−pitment interactions, *J. Biol. Chem. 277*, 36253−36261.
136. Schmid, V. H. R., Potthast, S., Wiener, M., Bergauer, V., Paulsen, H., and Storf, S. (2002) Pigment binding of Photosystem I light-harvesting proteins, *J. Biol. Chem. 277*, 37307−37314.
137. Morosinotto, T., Breton, J., Bassi, R., and Croce, R. (2003) The nature of a chlorophyll ligand in Lhca proteins determines the far red fluorescence emission typical of photosystem I, *J. Biol. Chem. 278*, 49223−49229.
138. Melkozernov, A. N., Schmid, V., Schmidt, G. W., and Blankenship, R. E. (1998) Energy redistribution in heterodimeric light-harvesting complex LHC I-730 of Photosystem I, *J. Phys. Chem. B 102*, 8183−8189.
139. van Amerongen, H., and van Grondelle, R. (2001) Understanding the energy transfer function of LHCII, the major light-harvesting complex of green plants, *J. Phys. Chem. B 105*, 604−617.
140. Ihalainen, J. A., Jensen, P. E., Haldrup, A., van Stokkum, I. H. M., van Grondelle, R., Scheller, H. V., and Dekker, J. (2002) Pigment organization and energy transfer dynamics in isolated photosystem I complexes from *Arabidopsis thaliana* depleted of the PSI-G, PSI-K, PSI-L, or PSI-N subunits, *Biophys. J. 83*, 2190−2201.
141. Ihalainen, J. A., van Stokkum, I. H., Gibasiewicz, K., Germano, M., van Grondelle, R., and Dekker, J. P. (2005) Kinetics of excitation trapping in intact Photosystem I of *Chlamydomonas reinhardtii* and *Arabidopsis thaliana*, *Biochim. Biophys. Acta 1706*, 267−275.
142. Melkozernov, A. N., Kargul, J., Lin, S., Barber, J., and Blankenship, R. E. (2005) Spectral and kinetic analysis of the energy coupling in the PSI-LHCI supercomplex from the green alga *Chlamydomonas* reinhardtii at 77 K, *Photosynth. Res. 86*, 203−215.
143. Wehner, A., Storf, S., Jahns, P., and Schmid, V. H. (2004) De-epoxidation of violaxanthin in light-harvesting complex I proteins, *J. Biol. Chem. 279*, 26823−26829.
144. Nield, J., Redding, K., and Hippler, M. (2004) Remodeling of light-harvesting protein complexes in *Chlamydomonas* in response to environmental changes, *Eukaryotic Cell 3*, 1370−1380.
145. Naumann, B., Stauber, E. J., Busch, A., Sommer, F., and Hippler, M. (2005) N-Terminal processing of Lhca3 is a key step in remodeling of the photosystem I-light-harvesting complex under iron deficiency in *Chlamydomonas reinhardtii*, *J. Biol. Chem. 280*, 20431−20441.
146. Ganeteg, U., Klimmek, F., and Jansson, S. (2004) Lhca5: An LHC-type protein associated with photosystem I, *Plant Mol. Biol. 54*, 641−651.
147. Storf, S., Stauber, E. J., Hippler, M., and Schmid, V. H. (2004) Proteomic analysis of the photosystem I light-harvesting antenna in tomato (*Lycopersicon esculentum*), *Biochemistry 43*, 9214−9224.
148. Klimmek, F., Ganeteg, U., Ihalainen, J. A., van Roon, H., Jensen, P. E., Scheller, H. V., Dekker, J. P., and Jansson, S. (2005) Structure of the higher plant light harvesting complex I: In vivo characterization and structural interdependence of the Lhca proteins, *Biochemistry 44*, 3065−3073.
149. Ihalainen, J. A., Klimmek, F., Ganeteg, U., van Stokkum, I. H. M., van Grondelle, R., Jansson, S., and Dekker, J. P. (2005) Excitation energy trapping in photosystem I complexes depleted in Lhca1 and Lhca4, *FEBS Lett. 579*, 4787−4791.
150. Holm, L., and Sander, C. (1991) Database algorithm for generating protein backbone and side-chain co-ordinates from a Cα trace. Application to model building and detection of co-ordinate errors, *J. Mol. Biol. 218*, 183−194.

BI051932O